Effects of Head-Supported Devices on Female Aviators During Simulated Helicopter Rides

Part I: Biomechanical Response

by Khalid W. Barazanji and Nabih M. Alem

Aircrew Protection Division

June 2000

USAARL

**U.S. Army
Aeromedical Research
Laboratory**

Notice

REPORT DOCUMENTATION PAGE

Form Approved
OMB No. 0704-0188

1a. REPORT SECURITY CLASSIFICATION Unclassified	1b. RESTRICTIVE MARKINGS

2a. SECURITY CLASSIFICATION AUTHORITY	3. DISTRIBUTION / AVAILABILITY OF REPORT Approved for public release, distribution unlimited
2b. DECLASSIFICATION / DOWNGRADING SCHEDULE	

4. PERFORMING ORGANIZATION REPORT NUMBER(S) USAARL Report No. 2000-16	5. MONITORING ORGANIZATION REPORT NUMBER(S)

6a. NAME OF PERFORMING ORGANIZATION U.S. Army Aeromedical Research Laboratory	6b. OFFICE SYMBOL (If applicable) MCMR-UAD	7a. NAME OF MONITORING ORGANIZATION U.S. Army Medical Research and Materiel Command

6c. ADDRESS (City, State, and ZIP Code) P.O. Box 620577 Fort Rucker, AL 36362-0577	7b. ADDRESS (City, State, and ZIP Code) 504 Scott Street Fort Detrick, MD 21702-5012

8a. NAME OF FUNDING / SPONSORING ORGANIZATION	8b. OFFICE SYMBOL (If applicable)	9. PROCUREMENT INSTRUMENT IDENTIFICATION NUMBER

8c. ADDRESS (City, State, and ZIP Code)

10. SOURCE OF FUNDING NUMBERS

PROGRAM ELEMENT NO.	PROJECT NO.	TASK NO.	WORK UNIT ACCESSION NO.
622787	878	Z	DA361535

11. TITLE (Include Security Classification)
Effect of Head-Supported Devices on Female Aviators During Simulated Helicopter Rides.
Part I: Biomechanical Response (U)

12. PERSONAL AUTHOR(S)
Dr. Khalid W. Barazanji and Dr. Nabih M. Alem

13a. TYPE OF REPORT Final	13b. TIME COVERED FROM_____ TO_____	14. DATE OF REPORT (Year, Month, Day) 2000 June	15. PAGE COUNT 55

16. SUPPLEMENTAL NOTATION

17. COSATI CODES			18. SUBJECT TERMS (Continue on reverse if necessary and identify by block number)
FIELD	GROUP	SUB-GROUP	Helicopters, females, head supported devices, aviation,
03/01			neck fatigue, neck strength, center of mass

19. ABSTRACT (Continue on reverse if necessary and identify by block number)

Researchers at the U.S. Army Aeromedical Research Laboratory (USAARL) recently concluded that weight-moment of head-supported devices (HSDs) worn by male aviators should not exceed 82.8 ± 22.9 Newton-centimeters (N-cm). The goal of this study was to define a safe range of weights and centers of mass of HSDs that can be tolerated by female helicopter pilots without affecting their health or degrading their performance. Twelve subjects were exposed to whole-body vibration while wearing an HSD with various mass properties. During exposure, biomechanical head acceleration, neck muscle activities, and performance responses were recorded. This paper reports the biomechanical response findings. Head pitch, anterior-posterior, and axial accelerations were measured for 12 different helmet configurations during sinusoidal vertical vibration having a magnitude of 0.45 m/s2 and frequencies swept from 2 Hz to 17 Hz at the rate of 0.25 Hz/sec. Results indicated that head pitch and axial acceleration levels for female subjects were lower than those for their male counterparts. This may be attributed to differences in seat damping
(continued)

20. DISTRIBUTION / AVAILABILITY OF ABSTRACT ☒ UNCLASSIFIED/UNLIMITED ☐ SAME AS RPT. ☐ DTIC USERS	21. ABSTRACT SECURITY CLASSIFICATION Unclassified	
22a. NAME OF RESPONSIBLE INDIVIDUAL Chief, Science Support Center	22b. TELEPHONE (Include Area Code) (334) 255-6907	22c. OFFICE SYMBOL MCMR-UAX-SS

DD Form 1473, JUN 86 Previous editions are obsolete. SECURITY CLASSIFICATION OF THIS PAGE

characteristics between the male and female studies as well as gender differences in neck muscle density. It was found that negative loading has a detrimental effect on females but not on males. Results also showed differences in magnitude of head pitch acceleration between weight moments higher and lower than 91.3 ± 28.6 N-cm, compatible to that recommended for their male counterparts (82.8 ± 22.9 N-cm). Based on the biomechanical response alone, it is recommended that the design criteria of HSDs mass properties should not be gender sensitive. However, further analysis of the physiological and performance responses need to be carried out prior to making a final recommendation.

Acknowledgments

Table of contents

Table of contents (continued)

Introduction

Aviators flying rotary-wing aircraft are exposed to whole-body vibration (WBV), transmitted primarily through the seating system causing musculoskeletal stress to the back and neck (Frymoyer et al., 1980; Gentlach, 1978). These stresses are aggravated when the head is further loaded with a helmet and other head-supported devices (HSDs) such as night vision goggles. New HSDs and improvements in crash protection technology and materials have altered the mass properties of modern aircrew helmets to an extent where existing operational and design criteria may no longer apply.

Safe and tolerable limits of HSD mass properties, such as mass location and distribution, are important design criteria for future aircrew helmets. The challenge for the Army research community is to establish those safe limits for HSD mass properties that can be tolerated by male and female aviators alike.

Phillips and Petrofsky (1983) examined the effects of 15 helmet configurations on the fatigue of neck muscles. They utilized a helmet simulator by adding three weights at five different center of gravity (CG) locations on the helmet. Six male subjects performed 30 minutes of right and left lateral rotation of the head while wearing one of the helmet configurations. Each subject then pulled against a load equivalent to 70 percent of his maximal voluntary contraction (MVC) and sustained this exertion until fatigue. Phillips and Petrofsky (1983) found, in general, that endurance time was sensitive to weight and CG location of helmet mass. They recommended that for a three-pound helmet, the optimal CG location should be at the forward position (5 cm in front of head/neck CG) and for a nine-pound helmet, the helmet CG should be behind head/neck CG. These recommendations were somewhat unexpected since helmet forward-loading strain and may fatigue the back neck muscles. These findings could be due to the small sample size of the six subjects.

A series of studies has been conducted at the U.S. Army Aeromedical Research Laboratory (USAARL) to evaluate the effects of HSD mass properties on biomechanical, physiological and performance responses of male pilots (Butler, 1992; Lantz, 1992; Alem, Meyer, and Albano, 1995). Butler (1992) showed a significant increase in head pitch acceleration response when the total head-supported load exceeded 83 N-cm relative to the atlanto-occipital complex (AOC). The AOC is a functional anatomic structure that represents the C0-C1-C2 joints of the upper cervical spine (Sobotta and Figge, 1974).

Alem et al. (1995) studied performance of male pilots under long exposure (up to 4 hours) to WBV and under four HSD configurations. They demonstrated that the subject's reaction time to a randomly appearing target increased as the weight moment of the helmet increased beyond 78 N-cm. Another USAARL study by Lantz (1992) showed significant changes in electromyography responses to HSD loading under WBV.

These USAARL studies concluded that the HSD weight moment should not exceed approximately 80 N-cm. Since this conclusion was derived from laboratory experiments with male volunteers as subjects, it was reasonable to expect that the limit would be different for

female aviators because of known gender differences in physiology, neck size, and upper body anthropometry (Gordon et al., 1989).

The main objective of the present study was to identify safe limits of HSD weight moments that can be tolerated by female aviators without adverse effects on their health and performance. Our approach was to measure and assess biomechanical, cognitive, physiological, and performance parameters associated with the exposure of female subjects to simulated helicopter vibration signatures and different helmet configurations. This report presents the results of the biomechanical analyses. Reports on all other results are in progress.

Methods

Subjects

Fifteen female subjects were recruited without coercion or bias. Two subjects (F06 and F10) withdrew from the study, one due to a leg injury and the other due to general fatigue. The data of the first subject (F01) were incomplete. Therefore, only the data of 12 subjects are considered in this report (Table 1).

Subjects were limited to non-aviation active duty females to avoid mixing subjects with different levels of helmet-wearing experience. In order to eliminate controllable sources of variation in the sample, the following subject selection criteria were applied:

- Body weight must be within Army standards for height and age.

- Must not participate regularly in specific neck and upper-body strengthening exercises.

- Must not have any significant medical condition as judged by the flight surgeon.

Table 1.
Anthropometric measurements for all subjects.

Subject	Age	Sitting height	Stature	Head breadth	Head circ	Head length	Menton top of head	Neck circ	Neck link	Bideltoid breadth	Weight
F02	39	86.7	162.6	13.9	52.4	18.0	18.0	31.7	11.1	39.9	57.3
F03	27	89.0	171.5	14.3	54.2	18.9	20.3	32.3	11.4	43.4	65.0
F04	30	79.5	160.7	14.9	56.7	19.3	19.9	35.2	9.1	43.3	69.6
F05	35	89.5	172.5	14.2	53.7	18.1	33.0	33.0	10.5	41.3	67.2
F07	35	84.4	165.1	15.2	56.9	19.5	21.2	34.0	14.0	41.4	66.8
F08	29	84.5	157.5	14.6	53.8	18.0	19.8	31.2	9.8	39.9	55.9
F09	20	86.8	165.1	15.3	56.2	19.2	19.3	33.0	11.8	41.0	59.1
F11	26	85.5	161.3	15.4	55.9	18.5	22.4	31.5	8.2	39.5	54.6
F12	40	88.0	177.8	14.4	55.5	19.0	21.7	32.3	9.9	42.3	68.2
F13	26	82.5	167.6	15.0	55.2	19.2	21.2	32.1	8.5	43.1	60.5
F14	34	84.6	160.0	14.9	54.0	18.3	19.7	34.8	9.5	43.5	68.2
F15	25	82.7	152.4	14.7	55.5	19.3	21.5	30.8	11.2	40.2	54.4
Mean	30.5	85.31	164.50	14.73	55.00	18.78	20.37	32.66	10.42	41.57	62.22
SD	6.11	2.91	7.03	0.47	1.37	0.56	1.25	1.40	1.61	1.51	5.84

All measurements are in cm. Weight in kg.

Instrumentation

Simulated HSD platform

To simulate various HSD weight moments, a modified aviator helmet was utilized for this study (Figure 1). This helmet allowed the investigators to vary weights and centers of mass (CM) precisely and rapidly. The helmet was calibrated for 5 weights (1.4 to 4.1 kg) and 21 CM locations (in the x, y, and z planes). This HSD simulator was used with success for male subjects in previous USAARL experiments and found to be adequate (Butler, 1992; Lantz, 1992; Alem et al., 1995). The appropriate locations of the weights were determined according to the method developed by Barazanji and Böhm (in progress).
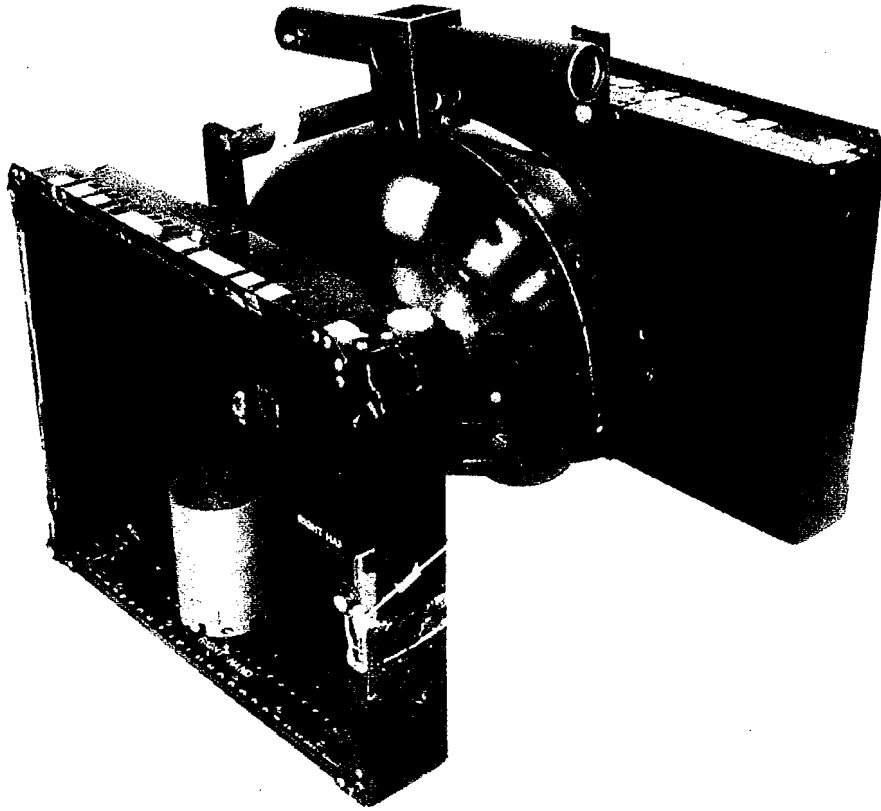
Figure 1. Side view of the helmet simulator.

Accelerometers/bite bar

Under WBV exposure, the head moves in a natural nodding motion in the mid-sagittal plane. This movement consists of two motions: linear motion in the superior-interior (axial) and anterior-posterior (AP) directions and angular motion in the pitch direction about the left-right axis. Since this was a three-degrees-of-freedom motion, at least three independent accelerometer readings were necessary to solve the kinematics problem. However, a fourth redundant accelerometer was added to simplify the equations and to obtain a robust solution. Thus, four miniature uni-axial accelerometers were mounted strategically on a bite bar (Figure 2).

The bite bar consisted of a precision-machined, lightweight, aluminum alloy mount approximately 12 cm long and attached to a U-shaped bite plate. This bite plate was fitted to the subject's teeth using dental molding compound one day prior to testing. The accelerometers (Entran model EGAXT) each measured approximately 5 x 4 x 8 mm with a dynamic range of 150 m/s^2. The bite bar was used during the swept sine vibration testing as explained below in the Procedures section.
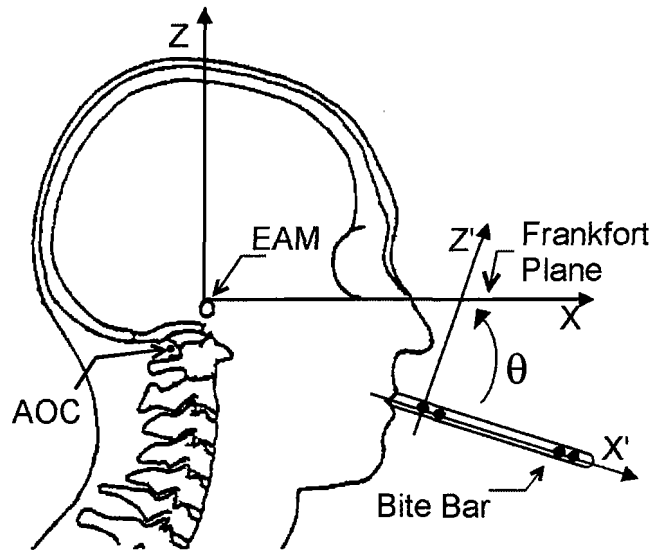
Figure 2.   Location of bite bar accelerometers with respect to EAM and AOC. EAM
             represents origin of the anatomical coordinate reference system XZ. θ is a
             pitch angle relating the bite bar coordinate system X'Z' to XZ. Filled circles
             on the bite bar represent locations of accelerometers. The X and Z axes
             denote the AP and axial directions, respectively.

Photogrammetry

     Bite bar position was acquired using the Optotrak (Northern Digital, Inc.) three-dimensional
(3D) position measurement system. This system operates by triangulating on pulsed infrared
light emitting diodes (LEDs), and yields 3D coordinates for each LED relative to a user-selected
viewing position. Two LEDs were added to the bite bar to measure bite bar position during the
swept sine sessions. From the position measurements, the contribution of gravity (1G) can be
subtracted from the acceleration measurements.

Procedures

General approach

     The general approach of the study was to measure head acceleration of female subjects in
response to swept sine vibration for 12 helmet configurations. This type of vibration allowed a
systematic method of characterizing the biomechanical response of the head under loading. The
12 helmet configurations were selected to reflect 3 helmet masses at 4 different CM locations.
This approach is a repeated measure design with two factors (helmet mass and helmet CM
location). In addition, the design was considered as a repeated measure with helmet weight
moment (product of helmet mass and helmet CM location) as the only factor.

     The subjects were exposed to the helmets based on a counterbalance design. Subject #1 was
tested according to the generalized sequence H_1 H_2 H_n H_3 H_{n-1} H_4 H_{n-2} H_5 etc., until

convergence ($H_\#$ = helmet configuration number, n = total number of helmets). That is, subject #1 was presented first with H_1, followed by H_2 H_{12} H_3 H_{11} H_4 H_{10} H_5 H_9 H_6 H_8, and H_7. Subject 2 was presented with the subsequent helmets, first with H_2, followed by H_3, H_1, H_4, H_{12}, H_5 etc. Subjects 3 - 6 had consecutive sequences. Subjects 7 - 12, however, were presented with the reverse order of helmet sequences than that of subjects 1 - 6. The rationale behind this arrangement was to present an equally balanced (albeit non-random) helmet presentation among all subjects. In addition, the number of helmets (n = 12) was chosen to allow comparisons to a similar study by Butler in 1992 that used the same HSD configurations on male subjects and showed significant levels.

The total number of subjects (n = 12) was based on a statistical design that had at least an 80 percent chance of achieving significant agreement between independent variables (weight moment) and dependent variables (head pitch acceleration) (Kraemer and Thiemann, 1987). Since each helmet test under swept sine took approximately 2 1/2 minutes, all 12 HSD configurations were tested in a single day. A no-helmet session always preceded the 12 helmet sessions for each subject, except for the last subject where the no-helmet case was the last session.

The actual location of the unloaded helmet CM relative to head CM was measured with a mass properties instrument (Deavers and McEntire, 1993). The head CM location relative to head AOC in the AP direction for the female subjects was chosen from the male study done by Butler in 1992. This allowed a comparison between results of this female study with results of the male study. The head CM location relative to head AOC for the male was multiplied by a ratio of 0.95 to reflect gender differences in head breadth and head length (Gordon et al., 1989). Using the Matlab program developed by Barazanji and Böhm (*in progress*), the actual locations of different loaded helmet CMs with respect to head AOC were estimated as shown in Table 2. The helmet weight moments were calculated as follows: weight moment [N-cm] = 9.806 $[m/s^2]$ × helmet mass [kg] × helmet CM relative to AOC in the AP direction [cm].

Prior to testing, the subjects were briefed on the testing procedure and signed a volunteer agreement affidavit. Also, a lateral x-ray of each subject's head was taken with the bite bar in her mouth. Radio-opaque pellets were used to mark the infra-orbital notch and the external auditory meatus (EAM). From the x-ray, the Frankfort plane-based anatomical reference frame was determined as shown in Figure 2. Also, the coordinates of the bite bar accelerometers with respect to the head AOC were measured.

The subject was seated in a UH-60 seat that was attached to the USAARL multi-axis ride simulator (MARS) platform. The bite bar was held rigidly in the subject's mouth during the test. Before each vibration session, the subject was asked to sit in an upright but a relaxed position.

Table 2.
Helmet mass properties for the swept sine vibration exposure.

	Helmet ID*	Design helmet mass (kg)	Design helmet CM forward distance relative to the head CM (cm)	Actual helmet mass (kg)	Actual helmet CM forward distance relative to the head CM (cm)	Actual helmet CM forward distance relative to the head AOC (cm)	Helmet weight moment relative to the head AOC (N-cm)
0	H00	No helmet					
1	H2-	2	-2	2.227	-2.76	0.29	6.3
2	H20	2	0	2.227	-0.65	2.40	52.6
3	H22	2	2	2.227	1.16	4.21	92.2
4	H24	2	4	2.227	2.97	6.02	131.9
5	H3-	3	-2	3.150	-2.40	0.65	20.0
6	H30	3	0	3.150	-0.38	2.67	82.5
7	H32 .	3	2	3.150	1.65	4.70	145.1
8	H34	3	4	3.150	3.67	6.72	207.7
9	H4-	4	-2	4.167	-2.55	0.50	20.5
10	H40	4	0	4.167	-0.67	2.38	97.3
11	H42	4	2	4.167	1.84	4.89	199.8
12	H44	4	4	4.167	3.72	6.77	276.6

* The first digit in the helmet ID reflects the intended (design) total weight of the helmet. The second digit represents the intended (design) location of the helmet CM relative to head CM in the AP direction. For example, H34 has a weight of 3 kg and the helmet CM is located 4 cm in front of head CM. The minus sign in the ID represents the helmet CM location as being 2 cm *behind* head CM. The number "2" is dropped from the ID for convenience. For example, H3- has a weight of 3 kg and the helmet CM is located about 2 cm behind head CM. The reason for this designation is to have compatible comparisons with Butler's male study (1992).

Sinusoidal whole-body vibration

WBV exposure was conducted on the USAARL MARS platform, to which a UH-60 seat was attached. Vibration levels did not exceed the exposure criterion for safe operation established by International Standards Organization guideline (ISO 2631, 1985). Input sinusoidal vibration was in the axial (vertical) direction and increased from 2 to 17 Hz at the rate of 0.25 Hz per second, then decreased back to 2 Hz at the same rate. A constant peak acceleration of approximately 0.4 G was maintained. The entire up/down sweep for each helmet load took approximately 2 minutes to complete.

Data analysis

Most of the data analysis was performed using Matlab, a high-performance language of technical computing (Mathworks, 1997). The acceleration signals were calibrated and filtered with a Butterworth 20-Hz low-pass filter that was designed based on the power spectral density (PSD) of the bite bar acceleration. As expected, 97 percent of the signal energy (i.e., the area under the PSD curve) occurred below 17 Hz, which was the highest input sinusoid frequency.

The filtered data were then resampled from 1000 Hz to 100 Hz so that they were compatible with the Optotrak sampling frequency of the bite bar position measurements. The bite bar pitch angle during the sinusoidal vibration was determined from the Optotrak position measurements. Using the pitch angle, the contribution of earth gravity (9.81 m/s^2) was subtracted from the resampled acceleration data.

Because of the exact registration with the subject's teeth, the head-bite bar system can be considered a rigid body, allowing the use of rigid-body kinematics to compute the linear and angular accelerations of the head motion. Further, the 3D motion of the head was mostly a nodding in the mid-sagittal plane so that 2D was assumed without a significant loss of accuracy. Two standard kinematics translations were applied to the "gravity-free" bite bar accelerations (standard kinematics textbooks; for example, see Bedford and Fowler, 1995): a linear translation from the bite bar to the head EAM in the axial and AP directions and a pitch rotation about the left-right axis as shown in Equations 1 and 2, respectively. From the x-ray, the axial and AP distances from the accelerometers to the EAM and the pitch angle between the bite bar reference frame and the Frankfort plane-based anatomical reference frame were determined (Figure 2). The x-ray readings and kinematics equations allowed pitch, axial, and AP accelerations of the head to be computed. To compare current findings with findings of Butler's 1992 study done on male subjects, head accelerations were determined at the atlanto-occipital complex.

$$
\begin{bmatrix} \mathbf{a}'_{x_0} \\ \mathbf{a}'_{z_0} \\ \alpha \\ \omega^2 \end{bmatrix} = \begin{bmatrix} 1 & 0 & +z_1 & -x_1 \\ 0 & 1 & -x_2 & -z_2 \\ 0 & 1 & -x_3 & -z_3 \\ 1 & 0 & +z_4 & -x_4 \end{bmatrix}^{-1} \begin{bmatrix} \mathbf{a}'_{x_1} \\ \mathbf{a}'_{z_2} \\ \mathbf{a}'_{z_3} \\ \mathbf{a}'_{x_4} \end{bmatrix}
\qquad \text{(Equation 1)}
$$

$$
\begin{bmatrix} \mathbf{a}_{x_0} \\ \mathbf{a}_{z_0} \end{bmatrix} = \begin{bmatrix} +\cos(\theta) & +\sin(\theta) \\ -\sin(\theta) & +\cos(\theta) \end{bmatrix} \begin{bmatrix} \mathbf{a}'_{x_0} \\ \mathbf{a}'_{z_0} \end{bmatrix}
\qquad \text{(Equation 2)}
$$

Where

$\mathbf{a}'_{x_1}$ = Magnitude of bite-bar accelerometer #1 in the x-direction (AP) [m/s^2],

$\mathbf{a}'_{z_2}$ = Magnitude of bite-bar accelerometer #2 in the z-direction (axial) [m/s^2]

$\mathbf{a}'_{z_3}$ = Magnitude of bite-bar accelerometer #3 in the z-direction (axial) [m/s^2],

$\mathbf{a}'_{x_4}$ = Magnitude of bite-bar accelerometer #4 in the x-direction (AP) [m/s^2],

x_i = AP distance between accelerometer #i and AOC in the bite-bar coordinate system [cm],

z_i = Axial distance between accelerometer #i and AOC in the bite-bar coordinate system [cm],

$\mathbf{a}'_{x_0}$ = AP acceleration magnitude at AOC in the bite-bar coordinate system [m/s^2],

$\mathbf{a}'_{z_0}$ = Axial acceleration magnitude at AOC in the bite-bar coordinate system [m/s^2],

α = Pitch acceleration of the head about the left-right axis [rad/s^2],

ω^2 = Angular velocity squared of the head about left-right axis [rad^2/s^2],

θ = Pitch angle relating the bite bar coordinate system X'Z' to Frankfurt coordinate system XZ (Figure 2),

$\mathbf{a}_{x_0}$ = AP acceleration magnitude at AOC in the Frankfurt coordinate system [m/s^2], and

$\mathbf{a}_{z_0}$ = Axial acceleration magnitude at AOC in the Frankfurt coordinate system [m/s^2].

Spectral analysis using the fast Fourier transform method was utilized to convert the time domain response of the platform acceleration, and head pitch, axial, and AP accelerations into the frequency domain. The mean power frequency (MPF) of the platform acceleration and the root mean square (RMS) of the head accelerations were computed. The peak magnitude at resonance was determined from the head RMS response, and the resonant frequency was determined from the acceleration MPF for different helmet configurations.

One-way analysis of variance (ANOVA) on the dominant resonant frequency and its magnitude was performed with the weight moment as a factor (n = 13) including the unloaded case (no-helmet). Two-way ANOVA was also applied to the resonant frequency and magnitude with the helmet weight as one factor (n = 3) and helmet CM position as the other factor (n = 4).

Tukey Honest Significant Difference Test was selected as our post hoc analysis. Other post hoc tests were also used such as Newman-Keuls Test (less restrictive), Scheffe Test (more restrictive), and Duncan Test (least restrictive). Only the results of the Tukey test are reported. Significance was identified when $p < 0.05$ was achieved. Marginal significance is also considered when the p value is between 0.05 and 0.1.

Results

The bite bar position was not measured during testing of the first subject, so it was not possible to correct the acceleration measurements for gravity. Thus the analysis was done on measurements of 12 subjects only.

Figure 3 shows an example of typical responses of the platform acceleration and the head accelerations of subject #5 for 12 helmet configurations. Note the symmetry in responses

9
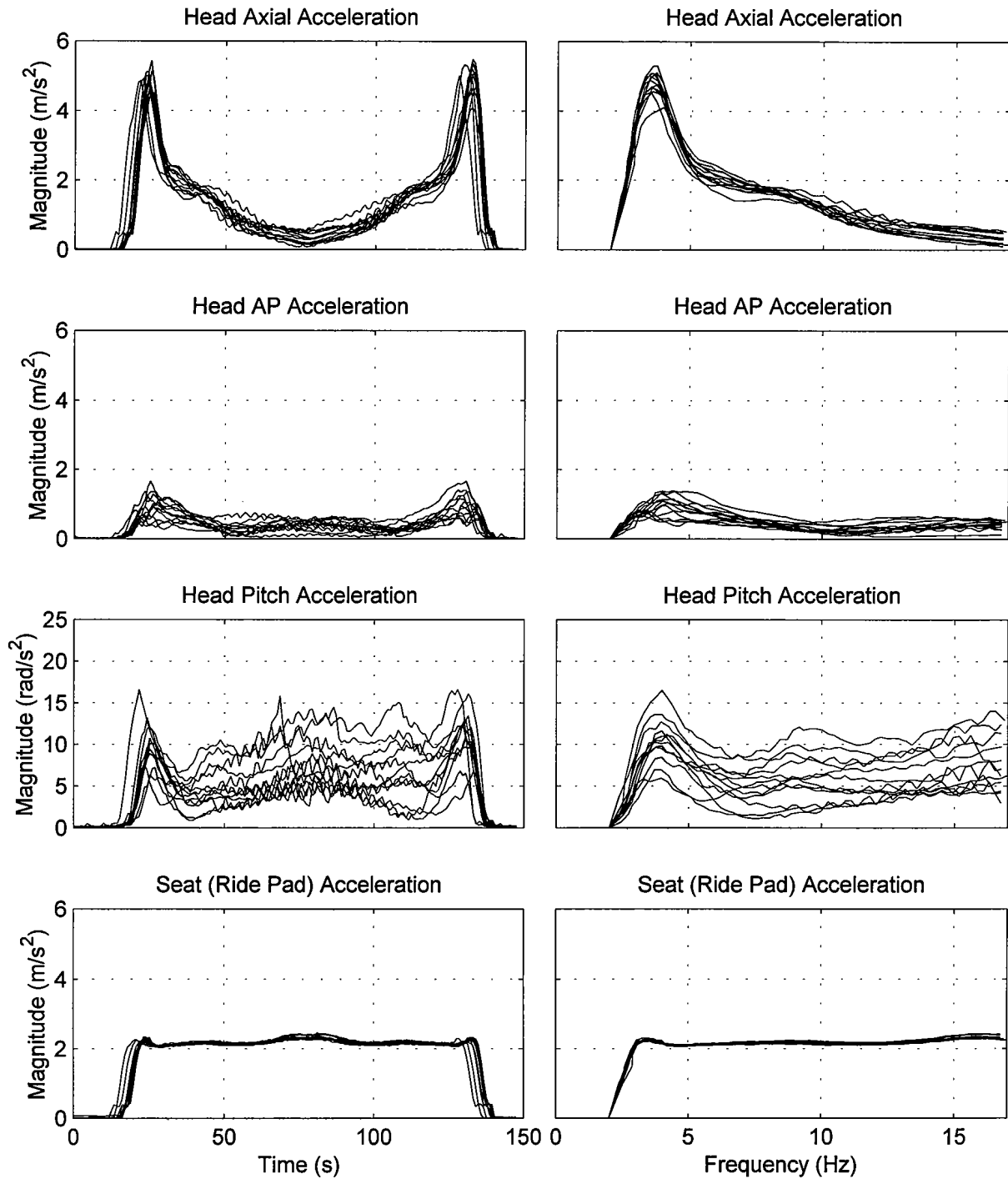
Figure 3. Head axial, head AP, head pitch, and platform axial accelerations as functions of vibration exposure time (left panels) and as functions of seat vibration frequency (right panels) for subject # 5 over 12 helmet loads.

Figure 4. Magnitude and frequency at first resonance for head axial, head AP, and head pitch accelerations plotted as functions of helmet weight moment for subject # 5. The filled circles represent the loaded cases and the "X" represents the unloaded case.

Figure 5. Magnitude and frequency at first resonance for head axial, head AP, and head pitch accelerations plotted as functions of helmet weight moment. The filled circles represent the loaded cases and the "X" represents the unloaded case averaged among all subjects. Error bars are +/- standard errors.

12

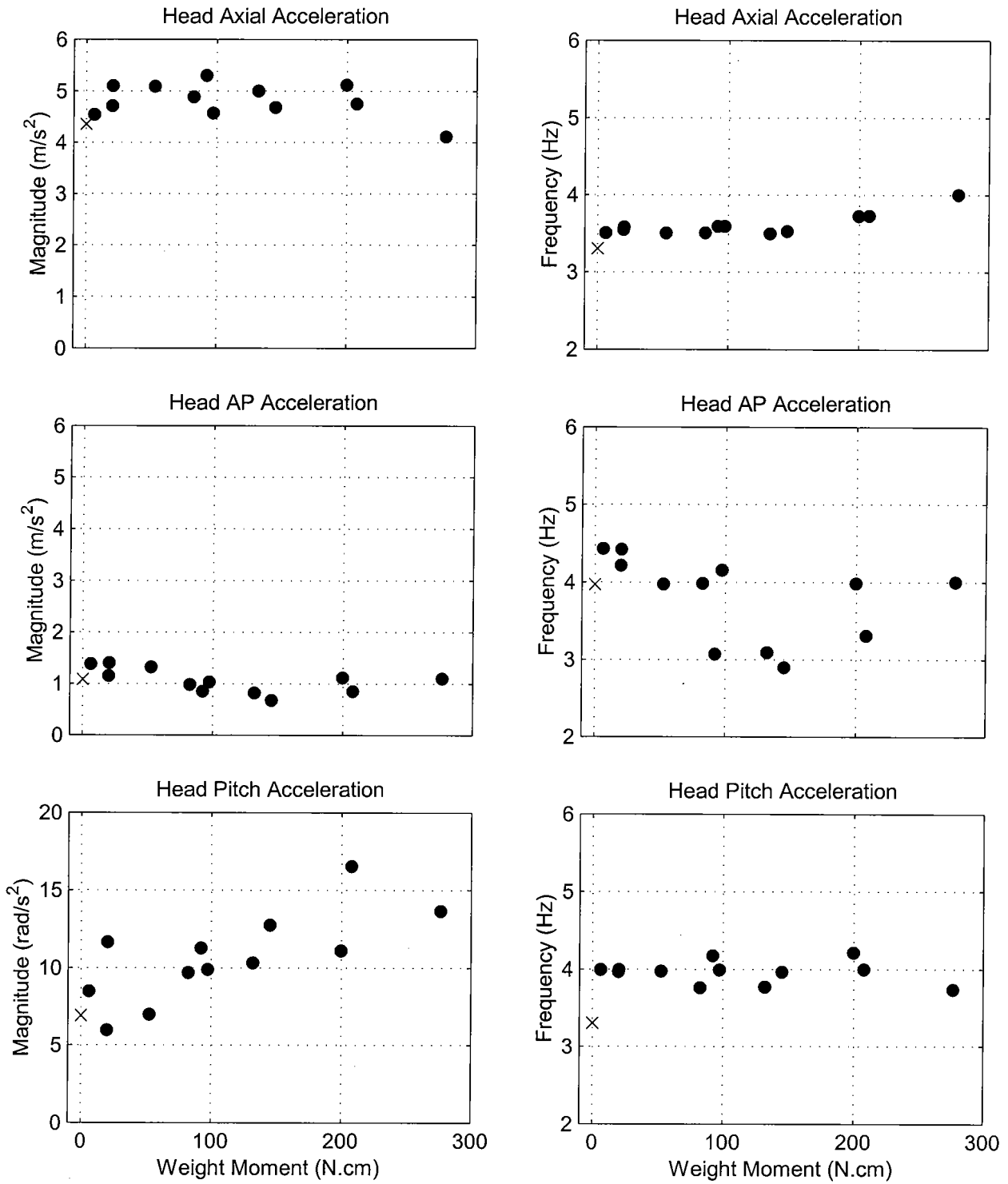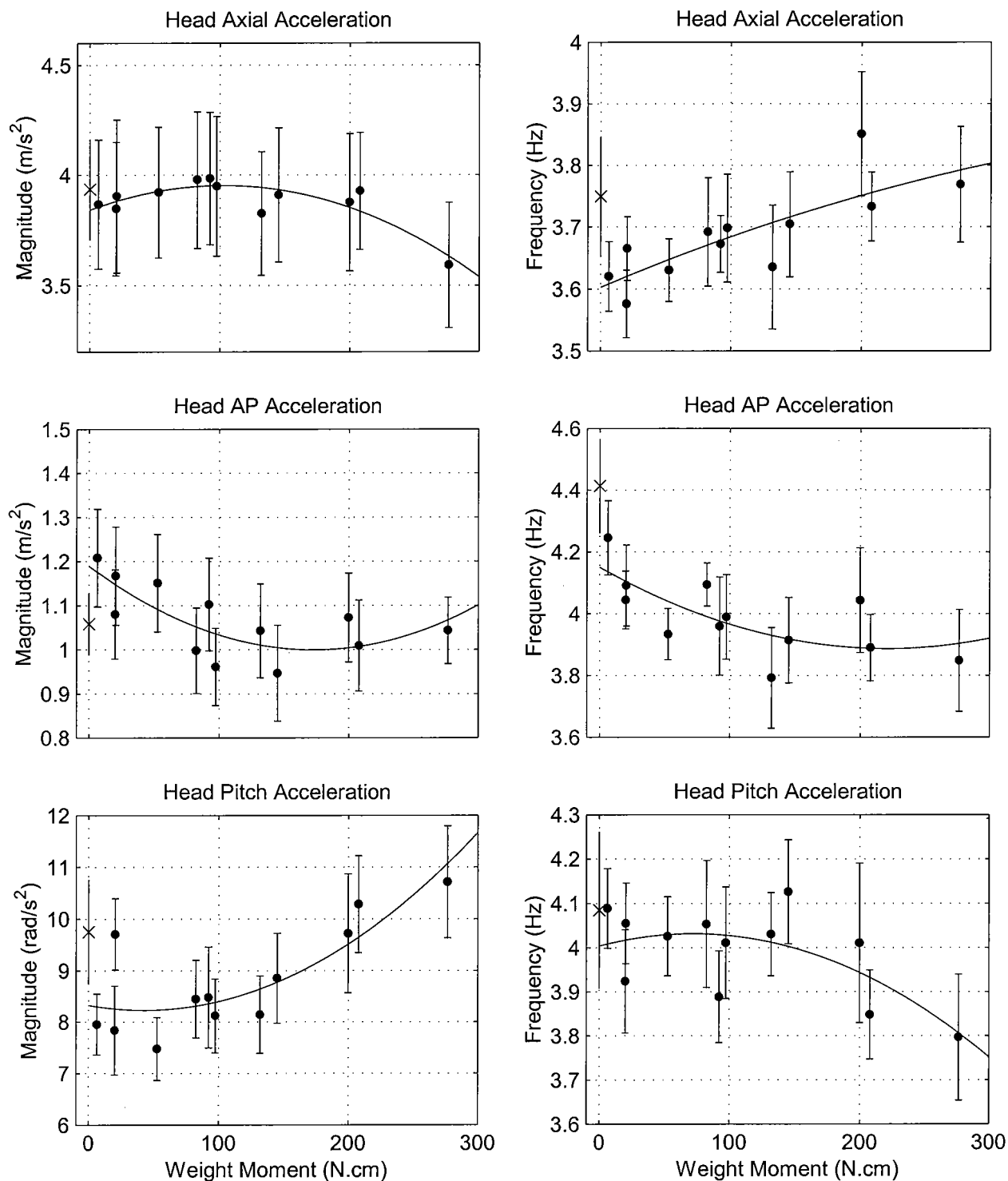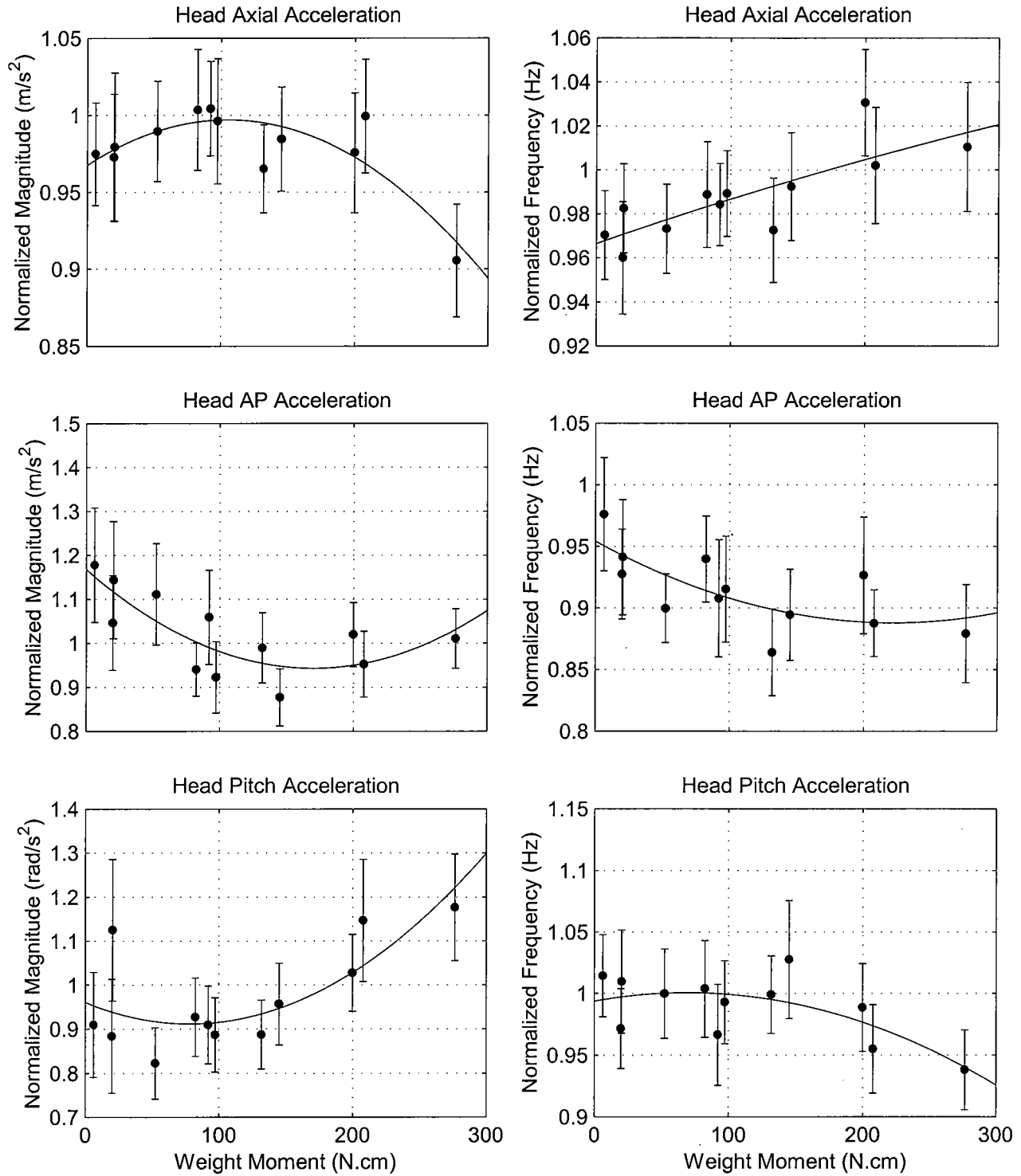Figure 6. Normalized magnitude and frequency at first resonance for head axial, head AP, and head pitch accelerations plotted as functions of helmet weight moment. Each normalized value represents the loaded case divided by the the unloaded case averaged among all subjects. Error bars are +/- standard errors.

between ramp-up and ramp-down phases of the swept sine vibration among all helmet configurations. This allowed averaging the magnitude for both phases of vibration, which was plotted against the input frequency of platform acceleration (Figure 3). All the acceleration responses for all the subjects are shown in Appendix B.

Although there was more than one resonant frequency, the first one was considered for this analysis because it was the most dominant. The first resonant frequency and its magnitude were extracted for each helmet load and for each subject. Figure 4 shows the first resonant frequency and magnitude of head axial, AP, and pitch accelerations for subject #5, as functions of helmet weight moment relative to AOC. Appendix C lists all the frequency and magnitude acceleration responses for all the subjects.

One-way ANOVA tests of weight moment

Figure 5 depicts the first resonant frequency and magnitude of head axial, AP, and pitch accelerations averaged among all subjects (n = 12), and plotted against weight moment. Another method of averaging among subjects is to normalize the loaded values by the unloaded one (i.e., no helmet case) for each subject, then, to average the normalized values among all subject. The plots of normalized values are shown in Figure 6. All responses in Figures 5 and 6 were fitted with a second order polynomial. The correlation coefficients for these curves were significant except for head AP acceleration frequency. Among acceleration magnitudes, head pitch acceleration has the highest correlation coefficient of 0.748 (p = 0.005).

One-way ANOVA was performed on the acceleration responses of Figure 5 with weight moment as the independent factor (n = 13). Differences in magnitude of pitch acceleration were found among helmets with a p-value of 0.00002 (F = 4.292) compared to other responses. The Tukey post hoc test was applied to the pitch acceleration magnitude with weight moment as the only repeated measure variable (n = 13). There was no significant difference between the unloaded case and any loaded session. Furthermore, significant differences between pitch acceleration magnitudes of the following helmets were identified: H44 different from H2-, H20, H24, H3-, and H40; H34 different from H2-, H20, and H3-.

Similarly, one-way ANOVA showed significant differences (p = 0.0006, F = 3.256) in normalized pitch acceleration magnitudes (Figure 6) due to helmet weight moment (n = 12). Normalization was with respect to each subject's unloaded value; hence, the sample size for this factor (n) is 12 rather than 13.

One-way ANOVA showed significant differences in axial acceleration magnitude (p = 0.0176, F = 2.215) and marginal significance in AP acceleration magnitude (p = 0.0520, F = 1.855) due to weight moment (n = 12). Post hoc tests were done on the axial and AP acceleration magnitudes using the helmet weight and CM position as the two repeated measures as shown in the next section.

14

Two-way ANOVA tests of helmet weight and CM location

Two-way ANOVA was also performed on the acceleration responses plotted in Figure 5 with helmet weight as one factor (n = 3) and helmet CM position as the other factor (n = 4) (Table 2). Results showed that there were marginal differences (p = 0.053, F = 2.835) in head axial acceleration magnitude due to helmet CM location (n = 4). This significance was mainly due to axial magnitude of H44 being significantly lower than those of all other helmets except H24 and H3-. No other differences in axial acceleration were found between other helmets. The mean and SD of axial acceleration magnitude among all helmets and subjects was 3.88 ± 0.1 m/s^2. Two-way ANOVA also indicated that there were marginal significant differences in AP acceleration magnitude (p = 0.067, F = 3.049) due to helmet weight (n = 3) only. No further analysis was performed on the AP acceleration response since the variation in the magnitude was very small (0.08 m/s^2) among all subjects and helmets.

The pitch acceleration magnitude data were rearranged and plotted in Figure 7 (left panel) against helmet weight and CM relative to head AOC. Figure 7 also shows the distribution of helmet weight moment versus helmet weight and CM location relative to head AOC.

Head pitch acceleration magnitude showed differences due to helmet weight (p = 0.000179, F = 13.107) and marginal differences due to helmet CM location (p = 0.064, F = 2.667). The interaction of helmet CM location and weight was also found significant for head pitch acceleration (p = 0.00276, F = 3.767).
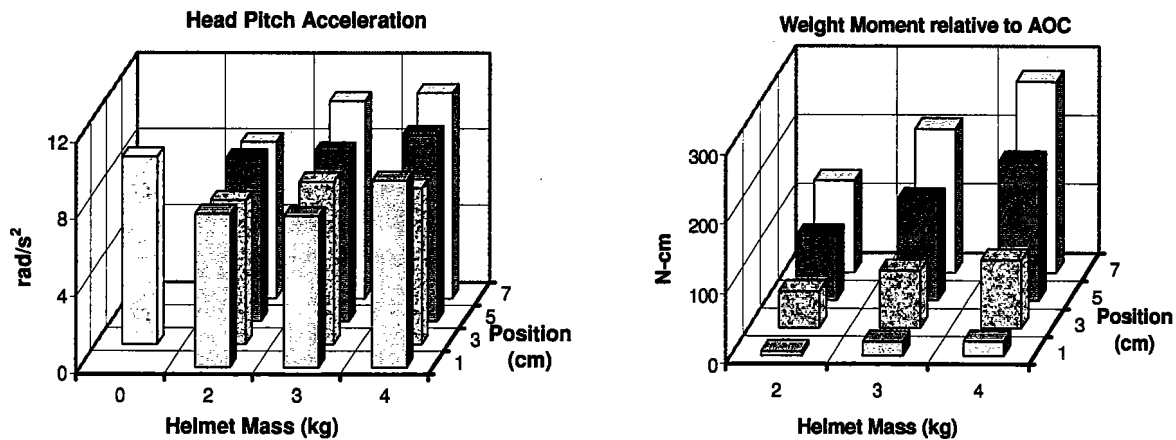

Figure 7. Head pitch acceleration (left panel) and helmet weight moment (right panel) are displayed against helmet mass and helmet CM (relative to head AOC). The unloaded (no helmet) case is also shown as the zero mass helmet.

The differences in frequency responses due to helmet CM and weight, although significant, are all within 1 Hz for all helmets and subjects, and thus not important. Furthermore, based on the previous ANOVA results, the pitch acceleration magnitude is the only significant response among the acceleration magnitudes. Therefore, the two-way post hoc analysis was performed only on the head pitch acceleration magnitude.

Table 3 shows the results of the Tukey test applied to the pitch acceleration magnitude data. The table is divided in such a way to reflect the two repeated measure factors, namely, helmet weight and CM position. For example, the first four rows (or 4 columns) represent p values as a result of Tukey test among helmets with weights of 2 kg and various CM position. Figures 8 and 9 show the pitch acceleration magnitude plotted as a 2D chart with all possible interaction scenarios between the design factors. The figures show the pitch acceleration magnitude averaged among helmet CM positions at each weight (Figure 8, right plot) and averaged among helmet weights at each CM position (Figure 9, right plot).

Table 3.
Post hoc Tukey Test (p values) on the pitch acceleration magnitude
with helmet weight and CM position as repeated measure factors.

	H2-	H20	H22	H24	H3-	H30	H32	H34	H4-	H40	H42	H44
H2-		0.9966	0.9924	1.0000	1.0000	0.9953	0.7380	0.0004	0.0174	1.0000	0.0160	0.0001
H20	0.9966		0.5898	0.9520	0.9997	0.6320	0.1470	0.0001	0.0007	0.9626	0.0006	0.0001
H22	0.9924	0.5898		0.9999	0.9643	1.0000	0.9996	0.0122	0.2824	0.9998	0.2685	0.0006
H24	1.0000	0.9520	0.9999		0.9999	1.0000	0.9303	0.0012	0.055*	1.0000	0.052*	0.0002
H3-	1.0000	0.9997	0.9643	0.9999		0.9744	0.5712	0.0002	0.0081	1.0000	0.0074	0.0001
H30	0.9953	0.6320	1.0000	1.0000	0.9744		0.9993	0.0101	0.2514	0.9999	0.2385	0.0005
H32	0.7380	0.1470	0.9996	0.9303	0.5712	0.9993		0.1107	0.7942	0.9143	0.7788	0.0083
H34	0.0004	0.0001	0.0122	0.0012	0.0002	0.0101	0.1107		0.9832	0.0011	0.9859	0.9986
H4-	0.0174	0.0007	0.2824	0.055*	0.0081	0.2514	0.7942	0.9832		0.0484	1.0000	0.5778
H40	1.0000	0.9626	0.9998	1.0000	1.0000	0.9999	0.9143	0.0011	0.0484		0.0450	0.0001
H42	0.0160	0.0006	0.2685	0.052*	0.0074	0.2385	0.7788	0.9859	1.0000	0.0450		0.5964
H44	0.0001	0.0001	0.0006	0.0002	0.0001	0.0005	0.0083	0.9986	0.5778	0.0001	0.5964	

* p values represent marginal significance. Shaded p values represent significance. See Table 1 for helmet symbol explanation.
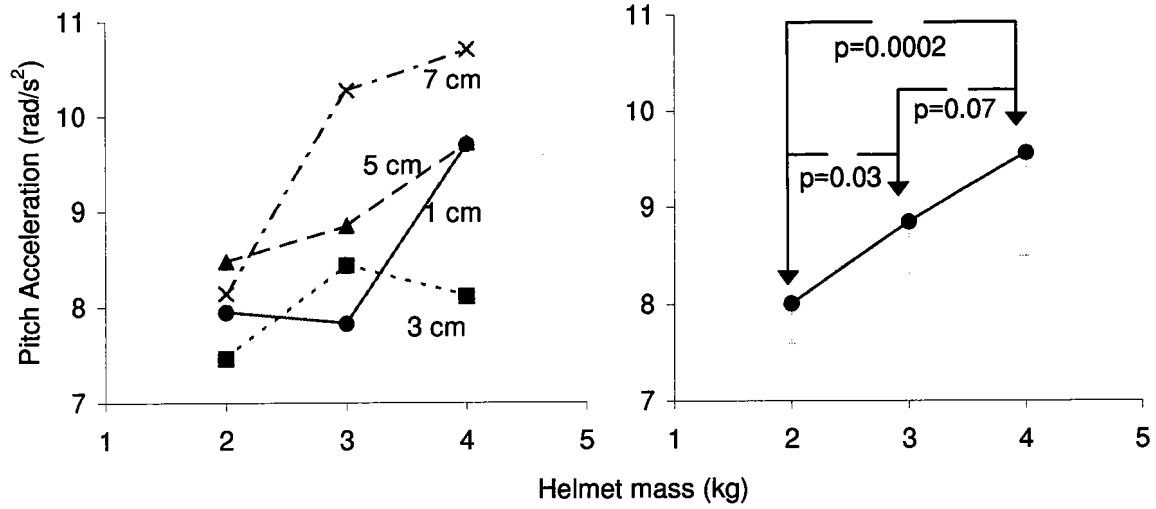
16

Figure 8. Pitch acceleration magnitude versus helmet mass. Averaged among 12 subjects for each helmet CM position relative to head AOC (left plot) and averaged for all helmet CM positions (right plot). Error bars are standard deviation (SD).
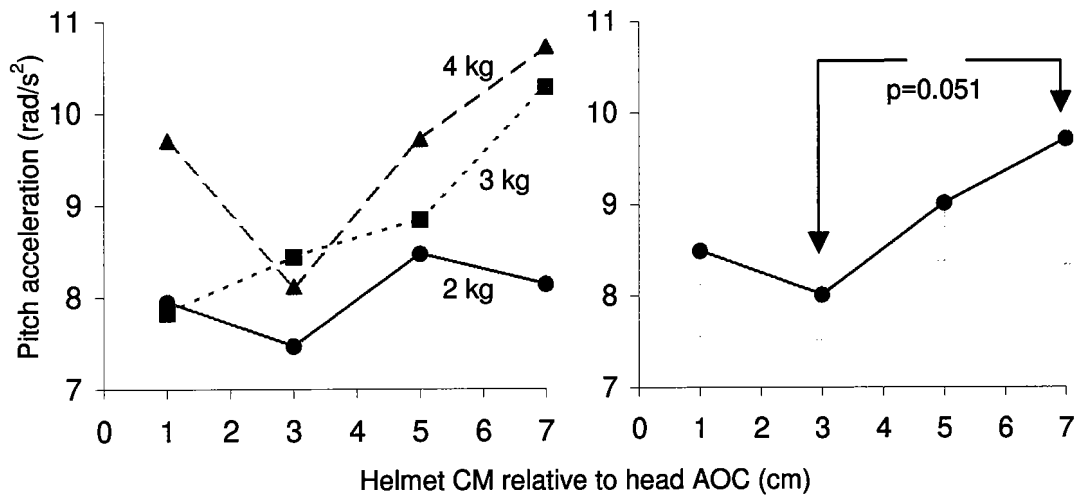

Figure 9. Pitch acceleration magnitude versus helmet CM position. Averaged among 12 subjects for each helmet mass (left plot) and averaged for all helmet masses (right plot). Error bars are SD.

Let H[*wt, #*] represent pitch acceleration magnitude averaged among all helmet weights (*wt*) at a specific helmet CM position relative to head CM (#). Also let H[*#, pos*] represent pitch acceleration magnitude averaged among all helmet CM positions relative to head CM (*pos*) at a specific helmet weight (#). It was found from the Tukey test that H[4, *pos*] is different from H[2, *pos*] (p = 0.0002) and marginally different from H[3, *pos*] (p = 0.0714) as shown in Figure 8, right plot. H[3, *pos*] was also found to be different from H[2, *pos*] (p = 0.0286). The Tukey test indicates that H[*wt*, 4] is marginally different from H[*wt*, 0] (p = 0.0511) but not different from those of H[*wt*, 2] and H[*wt*, -2] (Figure 9, right plot). No significant differences were found between H[*wt*, 2], H[*wt*, 0], and H[*wt*, -2].

Two-way ANOVA indicated that pitch acceleration normalized by the unloaded case changed significantly due to helmet weight (p = 0.00009, F = 14.67). No significance was found due to helmet CM position, but differences in normalized pitch magnitude was found due to the interaction between helmet weight and helmet CM position (p = 0.0060, F = 3.36). The Tukey test revealed less significant levels for the normalized pitch than the absolute pitch magnitude reported above. Significant differences between pitch magnitudes of the following helmets were identified: H44 different from H2-, H20, H22, H24, H3-, H30, H32, and H40; H42 different from H20; H40 different from H34; H4- different from H2-, H20, H22, H24, H3-, and H30; and H34 different from H2-, H20, H22, H24, H3-, and H30.

The pitch acceleration magnitude data were normalized by each subject's stature. The previous two-way ANOVA and post hoc tests were applied to the normalized pitch magnitude data. Although the p values were different than those reported for the un-normalized data, the significance levels due to helmet weight and CM position remained the same. Similar analysis was also done for pitch acceleration magnitude normalized by the subject's sitting stature and her neck link, separately. The significance levels also remained unchanged. The pitch data were also normalized by the subject's body surface area (BSA), which is defined by Guyton (1976) as

$$BSA = Weight^{0.425} \times Height^{0.725} \times 0.007184 \qquad (3)$$

No difference from original (un-normalized) findings was noted except that pitch acceleration magnitude normalized by BSA for H34 was marginally different from that for H32 (p = 0.0857). This marginal significance between H34 and H32 was not present in the un-normalized pitch acceleration.

Discussion and conclusions

Platform vibration in the axial (vertical) direction was transmitted through the seat to the musculoskeletal system of the subject, causing involuntary head motion. Combined with the loading of HSDs, this head motion might fatigue the pilot and degrade performance. For all subjects, RMS magnitude responses of the head axial, AP, and pitch accelerations to ramp-up swept sine were similar to the ramp–down portion of the swept sine. In addition, the magnitude of the platform acceleration remained fairly constant throughout all 12 sessions. Head pitch

acceleration response was found to be more sensitive to helmet loading than head AP or axial acceleration responses. All subjects exhibited similar responses.

Acceleration magnitude changed consistently with respect to the input vibration among all helmets and for all subjects (Appendix B). In general, the resonant frequency of the head accelerations remained unchanged. Two resonant frequencies can be clearly identified from the head axial acceleration response. The first resonant frequency ranged between 3.5 - 4.5 Hz and the second ranged between 7 - 8 Hz. These findings were in agreement with those of Butler's study involving male subjects. The results were also in agreement with Wilder et al. (1982) who identified a resonant frequency of 4.9 and 4.75 Hz of vibration transmissibility measured at the top of the head of seated male and female subjects, respectively. Similarly, Paddan and Griffin (1988) reported a resonance frequency of 4 - 6 Hz of head accelerations during vertical seat vibration.

Head axial acceleration

Peak head axial acceleration (at first resonance) tends to be insensitive to changes in helmet weight moments with respect to AOC. This finding agrees with Butler (1992), who concluded that head axial acceleration at the AOC for the male subjects did not change significantly as helmet CM and mass changed. However, head axial accelerations for all female subjects ranged between 3 - 4.5 m/s^2, lower than the range of approximately 6 - 7 m/s^2 for the male subjects. This gender distinction was true for all helmet configurations as well as for the unloaded case. However, the vertical vibration transmissibility factor from the seat to the head for female subjects was found to be in the range of 1.65 − 1.8 similar to that reported by Wilder et al. (1982) for females (1.62±0.2). In our study, there was a drop of approximately 50 percent in the vibration transmission from the platform to the seat. This may be attributed to the damping introduced by the seat cushion and the seatpad itself (that contains the accelerometer). Butler (1992) reported a vertical transmissibility factor of more than 2 at the head. In that study, the accelerometer was placed underneath the seat; whereas, in this study, the accelerometer was placed above the seat (input vibration to the spinal system). Although the male subjects in Butler's study were seated on a cushioned and stiffened seat, it may be possible to have a different damping characteristic to the seat used in this study.

In comparing head acceleration values between studies, several factors that should carefully be considered include seated posture, seat characteristics (e.g. bottom cushion, backrest cushion, angle of seatback), whether subjects used lap and/or shoulder belts, location of head accelerometers, and correcting the acceleration measurements for the vertical component of earth gravity.

The correction for earth gravity is often ignored (Paddan and Griffin 1988) or not addressed (Wilder et al., 1982; Butler, 1992) by most researchers. In this study, the vertical component of earth gravity was subtracted from the head acceleration measurements. From the solution of Equation 1, earth gravity does not contribute to pitch acceleration calculation at all. Sensitivity analysis was conducted to determine the percent of error in omitting earth gravity contribution. Although, as expected, this analysis showed pitch acceleration insensitivity to earth gravity

contribution, axial and AP accelerations mildly increased by 5 percent when earth gravity contribution was omitted. Coincidently, magnitudes of axial and AP accelerations at resonance exhibited little or no change due to helmet load. Therefore, no significant change in axial and AP accelerations was found due to earth gravity contribution. Nevertheless, the contribution of earth gravity should be considered if greater variations in axial or AP accelerations are expected due to, for example, gender, age, or different environments (ground versus flight).

Another important factor in vibration transmission from seat to head is the seat characteristics. Wilder et al. (1982) appeared not to use a backrest and the seat appeared not to have cushions (although not mentioned in the publication, it appeared from a picture of a seated subject that the seat was rigid). Paddan and Griffin (1988) used two types of seats, one with a rigid backrest and one without. No lap or shoulder belts were used. They partly attributed increased head AP and axial accelerations when using a rigid backrest to the additional transmission path for vibration. However, their results showed that head pitch acceleration changed insignificantly between the two seats. Butler (1992) used a cushioned seat with backrest but strapped the subjects using both lap and shoulder belts. No details were given whether the backrest was cushioned. In this study, a cushioned seat with a cushioned backrest was used. Since Optotrak LED markers were attached to the subject's T1 location, an additional backrest cushion was utilized. The double backrest cushion might have added more damping to the vibration transmission from the seat to the head, according to the findings by Paddan and Griffin (1988). Thus different seat characteristics among studies will have different damping effects on the head acceleration transmissibility.

The position of the subject's feet was not controlled in this study. However, there is no evidence that this factor significantly altered head acceleration.

The location of head accelerometers is another, if not the most, important factor in comparing head acceleration responses between studies. In this female study and in Butler's (1992) male study, bite-bar acceleration measurements were translated to the head AOC. However, the motion equations were utilized differently. In addition, Butler (1992) used another group of subjects to determine an average location of AOC relative to head EAM; whereas, in our study, this was done separately for each subject. This is an important difference between this female study and Butler's (1992) male study in interpreting and comparing gender-head responses to vibration and HSD loading. Paddan and Griffin (1988) reported their head acceleration findings at the mouth using a bite-bar and Wilder et al. (1982) measured head acceleration at the top of the head; hence, no mathematical translation of bite-bar acceleration to a more anatomically related-location on the head was utilized such as the AOC or EAM. Thus, it is evident from previous studies and the current one that an anatomical landmark on the head needs to be defined and used as a reference point in future head transmissibility studies. This issue will be addressed in a USAARL report by Haley and McEntire (*in preparation*).

Head AP acceleration

Butler (1992) showed that head AP acceleration for male subjects was insensitive to helmet loading. For the female subjects, there was little change in the magnitude of head AP

acceleration due to helmet weight moment (Figure 4). In addition, the female AP acceleration had a mean and SD of 1.07 and 0.08 m/s^2, respectively, similar to the accelerations seen in male subjects.

Head pitch acceleration

Analysis based on the data shown in Figures 5 and 6 suggests that the magnitude of head pitch acceleration is the most sensitive parameter to changes in helmet weight moment. This is in general agreement with Butler's findings for male subjects. Furthermore, ANOVA tests reveal that helmet weight is a more significant factor than helmet CM position in changing pitch acceleration (Figures 8 and 9).

In general, two-way ANOVA showed more significance levels than the one-way ANOVA. No significance was found between the unloaded case and any helmet run for the pitch magnitude response. This was somewhat unexpected but may be explained by the fact that the unloaded case unintentionally was not considered in our counterbalance design of helmet sequences (see general approach section); hence, the unloaded session was always the first run for each subject except for the last subject. This may also explain the large SD of the unloaded case (36 percent of the mean). Although not significant, pitch acceleration for the unloaded case was higher than that for H20, H30, H40, H2-, and H3-. Butler (1992) found similar findings for the male aviators but not significant. It is conceivable that because the magnitude of pitch acceleration for males is about 50 - 100 percent higher than females, the differences between loaded and unloaded cases are more pronounced. An important gender similarity, however, is that the unloaded case was not significantly different from H4-, suggesting that H4- may present a balanced or negative head loading. Balanced head loading means that the sum of all weight moments about the head pivot point is equal to zero, whereas negative head loading means the load is behind the head pivot point or center of rotation.

Pitch acceleration for H4- (4 kg with a CM at approximately 2 cm behind head CM) was found to be significantly higher than that for H40 and H3-. These findings indicate that H4- applies a negative weight moment on the pivot point of the head. Since H4- is located 1.55 cm behind EAM and 0.45 cm in front of AOC, the center of rotation cannot be the AOC identified by Butler (1992), which is 2.05 cm behind EAM but rather closer to EAM (< 1.55 cm behind EAM). An attempt to locate this functional pivot point is described in Appendix A. Based on the rational and calculations in Appendix A, the new head pivot point position was calculated and found to be in the range of 0.77 – 0.96 cm behind EAM.

These upswings of pitch acceleration response from H3- to H4- and from H40 to H4- were also observed in the male aviator but were not significant (Butler 1992). This is an important gender difference, suggesting that negative head loading is more detrimental for females than males. During negative loading, the frontal neck muscles (e.g. sternocleidomastoid) should play the most active role in supporting the head. Thus the gender-difference for negative loading may be attributed to gender-differences in frontal neck muscular characteristics such as density and muscle fiber recruitment.

Despite the fact that the subject's upper body anthropometric measurements were not controlled in the selection criteria, their contribution to vibration transmission to the head were minimal. Normalization of pitch acceleration by anthropometric measurements (such as stature, sitting height, neck link or BSA) had little or no effect on the significance levels found in the absolute pitch acceleration (Table 3). In general, standard deviations of the anthropometric measurements were in the range of 3 - 6 percent of the mean (except for neck link, it was 15 percent), lower than that for pitch acceleration magnitude (about 15 percent of mean). Butler (1992) reported that the neck muscle electromyography (EMG) signal increased significantly with higher head load under vibration. Thus, neck and upper back muscle density may play a role in altering vibration transmissibility to the head. However, muscle density measurement is not available and cannot be derived from available anthropometric measurements obtained in this study.

Helmet operation limits

The results in Table 3 indicate that there is a region of heavier helmets where pitch acceleration was higher than that for the lighter helmet region. The heavier region included H44, H42, H34, and H32. Although, only the H32 showed a significant difference compared to H44 based on the Tukey test, other post hoc tests (i.e., Duncan test) showed that pitch acceleration for H32 was significantly different from H20, H3-, H34, H44 and marginally different from H2-, H4-, and H42. Thus, it is safer to include H32 with the heavier helmet group. The five helmet loads (i.e., H40, H30, H20, H22, and H24) that surround the heavy helmets can be selected as the upper safe limit of helmet weight moment. The weight moment among these helmets was averaged and found to be 91.3 ± 28.6 N-cm relative to AOC (or 34.83 ± 32.72 N-cm relative to EAM). This upper weight moment limit for the female is close to the 82.8 ± 22.9 N-cm limit (relative to AOC) for the male aviator, identified by Butler (1992). In fact, Butler identified the same safe helmet group (i.e., H40, H30, H20, H22, and H24) as in this study. The difference between the male and female limits is simply attributed to different helmet simulators (i.e., different mass properties) used in each study.

In general, because of gender differences in upper body anthropometry, it was expected to identify gender differences in helmet design criteria based on the biomechanical response. But comparing the averaged anthropometric measurements among the female subjects of this study (Table 1) and those for the male study, there are no appreciable differences except for the body surface area (the male BSA is about 20 percent higher than the female BSA). Thus, it is unlikely that these anthropometric measurements can explain gender acceleration differences. However, in order to investigate the effects of anthropometric dimensions accurately, gender comparisons should be done only after each subject's (male and female) acceleration magnitudes are normalized by a particular anthropometric value. Although individual male data were not available and the contribution of anthropometric dimensions was minimal within this female subject group (Table 1), the effects of anthropometric dimensions may be greater between the male and female groups.

Another method of presenting safe helmet operational limits is by plotting acceptable regions of tested mass and centers of mass with respect to the head EAM (Figure 10).
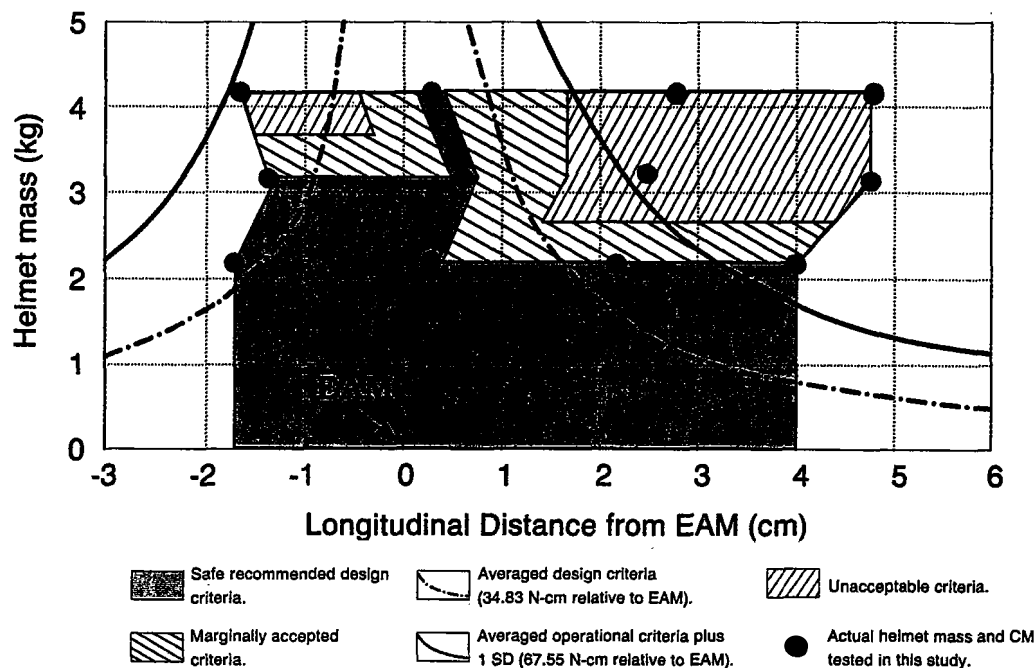
Figure 10. HSD operational design criteria for female subjects. Filled circles represent the actual helmet mass and CM tested in this study. The solid shaded region is the safe recommended design criteria, the back-slash regions are the marginally accepted criteria, and the forward-slash regions are the unacceptable criteria. The dashed curve represents the averaged design criteria (34.83 N-cm relative to EAM). The solid curve is the averaged operational criteria plus 1 SD (67.55 N-cm relative to EAM).

The regions in Figure 10 were identified based on the pitch acceleration results (Table 3, Figures 7 - 9). Note that the helmet CM's are presented with respect to EAM because the determination of head pivot point is not yet resolved and even not fully understood (i.e., is it AOC, COC, functional pivot point by this study, or other anatomical structures?). Also shown in Figure 10 is a region of marginal acceptance of HSD design values (back-slash regions). This region was arbitrarily selected as half of the distance between accepted and unaccepted mass and CM values. The solid shaded region represents the conservative operational criteria for female HSD mass properties whereas the back-slash regions represent the upper limit for the HSD mass design criteria. Figure 10 shows that the averaged conservative weight moment limit of 34.83 N-cm (dashed curve in Figure 10) and the averaged upper weight moment limit of 67.55 N-cm (solid curve in Figure 10) identified earlier may not agree with the shaded regions. Since the shaded regions are a more accurate representation of the findings of this study, averaged superimposed limits (curves in Figure 10) should only be used to extrapolate values outside the tested regions. The area between the superimposed curves represents the marginally accepted area (i.e., one standard deviation from the mean).

Figure 10 should be considered as a refinement to the USAARL longitudinal CM curve identified by Butler (1992) and summarized by McEntire and Shanahan (1998). For the positive helmet loading (helmet CM in front of head and neck CM), the maximum allowable weight moment is not gender sensitive. Although a difference in weight moment limit between this female study and that of Butler's male study (1992) was found, this difference was due to the usage of two different helmet simulators between both studies.

A new region of unacceptable operational criteria for HSD mass properties was identified for the female aviator that was not present for the male aviator. That is, the negative head loading relative to EAM (upper left forward-slash region of Figure 10). This finding may have an important implication regarding helmet counterbalance weights that aviators add on the back of their helmets. The purpose of these weights is to balance the helmet and HSD load by shifting the forward helmet CM back to the vicinity of their head and neck CM. As the helmet CM with counterbalance weights is closer to the head and neck CM, frontal neck muscles (e.g., sternocleidomastoid) become more active in balancing head loading. Thus, the female sensitivity to negative head loading suggests that their frontal neck muscles may not be sufficient in supporting the head in cases of fully equipped helmets with counterbalance weights.

Study limitations

The subjects were instructed to relax and not to resist natural head motion during exposure to sinusoidal WBV. However, there is a possibility that some subjects may have tensed up their neck muscle during vibration exposure. We recognized this factor from the beginning of the study and thus each subject had a familiarization session to minimize this factor. The subjects were frequently asked if they were relaxed during the helmet sessions and visually monitored for any inconsistencies regarding their reaction to the vibration and helmet load. Any significant voluntary neck muscle tensing would result in altering the head acceleration response curves among different helmet sessions for each subject. As shown in Appendix B and Figure 5, there was an excellent agreement among all subjects regarding their axial acceleration frequency and magnitude responses for all helmet sessions that was evident in the small standard deviation of 0.1 m/s^2 (or 2.4 percent of mean). This small variation in axial acceleration response among all subjects and helmets demonstrates that voluntary muscle tensing was negligible. Butler (1992) found that there was a stronger contraction of the trapezius muscle for the heavier helmets (weight moments > 138 N-cm). These findings suggest that the usage of neck EMG electrodes in this study might have not eliminated the doubts that the subjects were tensing up. However, we feel confident that the subjects were relaxed and voluntary muscle tensing was minimal.

Helmet fitting was a problem for subjects with a smaller head circumference (Table 1). Even though multiple layers of Thermal Plastic Liner (TPL) were added to the helmet, some subjects were complaining of hot spots at their forehead. There is a small possibility that heavy helmets such as the H44 were slightly slipping (changing its weight moment) during vibration for a subject with smaller head dimensions. This slippage is unlikely to have occurred because of the similarity of axial acceleration responses within these female subjects and in comparison with the male study.

24

Each subject was also exposed to random WBV (6 sessions) that spanned over 6 days. Each of these sessions involved neck muscle exertions as well as 90 minutes of exposure to random vibration, similar to that experienced in a UH-60 helicopter. There were some subjects who performed the acceleration sessions 30 - 45 min after a random vibration session, and there were others who performed the acceleration sessions on a separate day. The test schedule was not controlled due to conflicts with the subjects' prior engagements. Since head motion under WBV is a dynamic process involving involuntary muscle contraction, this uncontrolled test schedule may have slightly affected the results.

Recommendations

The results reported here suggest that head pitch acceleration for the female subjects is the most sensitive response to head-supported devices, compared with AP and axial accelerations. Based on this biomechanical response, we recommend that operational criteria for head-supported devices should follow the shaded areas of Figure 10. For extrapolation, the helmet weight moment for female aviators should not exceed the conservative upper-limit of 35 N-cm or the more relaxed upper limit of 68 N-cm, both relative to EAM (91 N-cm and 120 N-cm relative to AOC, respectively). Indeed, other parts of the study (i.e., neck EMG and performance responses) need to be analyzed in order to assure this recommendation. In general, the design criteria for head-supported devices based on head motion are similar for male and female aviators. However, further studies are needed to address head motion differences between male and female aviators wearing helmets with counterbalance weights.

References

Alem, N.M., Meyer, M.D., and Albano, J.P. 1995. Effects of head supported devices on pilot performance during simulated helicopter rides. Fort Rucker, AL: U.S. Army Aeromedical Research Lab. USAARL Report No. 95-37.

Barazanji, K.W., and Böhm, U. 2000. Test and Evaluation of the variable weight, variable CG helmet simulator. Fort Rucker, AL: U.S. Army Aeromedical Research Lab. USAARL report (*in progress*).

Bedford, A., and Fowler, W. 1995. Engineering mechanics-dynamics. Reading, MA: Addison-Wesley.

Butler, B.P. 1992. Helmeted head and neck dynamics under whole-body vibration. Ph.D. dissertation, University of Michigan, Ann Arbor, MI.

Deavers, M.B., and McEntire, B.J. 1993. An automated method for determining mass properties. Fort Rucker, AL: U.S. Army Aeromedical Research Lab. USAARL Report No. 93-4.

Frymoyer, J.W., Pope, M.H., Rosen, J.C., Goggin, J., Wilder, D.G., and Costanza, M. 1980. Epidemiologic studies of low-back pain. Spine. 5:419-423.

Gentlach, J.R. 1978. Response of the skeletal system to helicopter-unique vibration. Aviation Space and Environmental Medicine. 49:253-256.

Gordon, C.C., Thomas, C., Clauser, C.E., Bradtmiller, B., McConville, J.T., Tebbetts, I., and Walker, R.A. 1989. Anthropometric survey of U.S. Army personnel: Methods and summary statistics. Technical Report, Natick/TR-89/044.

Guyton, A.C. 1976. Textbook of Medical Physiology. W.B. Saunders, Philadelphia, PA.

Haley, J.L., and McEntire, B.J. 2000. Head and neck center-of-mass location relative to the ear canals. Fort Rucker, AL: U.S. Army Aeromedical Research Lab. USAARL report (*in progress*).

International Organization for Standardization. 1985. Guide for the evaluation of human exposure to whole-body vibration. ISO 2631.

Kraemer, H.C., and Thiemann, S. 1987. How many subjects? Statistical power analysis in research. Newbury Park, CA, SAGE Publications.

Lantz, S.A. 1992. Analysis of the effects of head-supported mass and random axial whole-body vibration on changes in neck muscle myoelectric activity, posture, and vigilance performance. Final report for contract #DABT01-92-P2326, USAARL.

<u>MATLAB 5</u>. 1997. Natick, MA. The MathWorks, Inc.

McConville, J.T., Churchill, T.D., Kaleps, I., Clauser, C.E., and Cuzzi, J. 1980. <u>Anthropometric relationships of body and body segment moments of inertia</u>. Wright-Patterson Air Force Base, OH: AF Aerospace Medical Research Laboratory. AFAMRL-TR 80-119.

McEntire, B.J., and Shanahan D.F. 1998. <u>Mass requirements for helicopter aircrew helmets</u>. Fort Rucker, AL: U.S. Army Aeromedical Research Lab. USAARL Report No. 98-14.

Paddan, G.S., and Griffin, M.J. 1988. The transmission of translational seat vibration to the head – I. Vertical seat vibration. <u>J Biomech</u>, 21(3): 191-197.

Phillips, C.A. and Petrofsky, J.S. 1983. Neck muscle loading and fatigue: Systematic variation of headgear weight and center-of-gravity. <u>Aviation, Space, and Environmental Medicine</u>. 54(10):901-905.

Sobotta, V., and Figge, F.H .J. 1974. <u>Atlas of human Anatomy</u>. Vol 1. NY: Hafner Press.

Wilder, D.G., Woodworth, B.B., Frymoyer, J.W., and Pope, M.H. 1982. Vibration and the human spine. <u>Spine</u>. Volume 7, Number 3.

Appendix A.

Determination of head center of rotation.

The findings in this study suggest that the loaded head was unbalanced due to the significant increase in pitch acceleration from H3- to H4- and from H40 to H4- (Table 3 and Figures 8 - 9). The head being balanced means that effective weight moment (combining head, neck and helmet) about the pivot point equals zero. Therefore, the weight moment of H4- exceeded that of the unloaded head relevant to the head pivot point (negative head loading). The center of rotation in this study is assumed to be at head AOC (2.05 ± 0.33 cm behind EAM). However, Haley and McEntire (1999) suggest that the combined head and neck CM is at center of the condyle (COC), which is about 0.2 cm behind EAM in the AP direction. They also indicated that COC is the head center of rotation for the nodding motion. According to the findings of this study, the pivot point should be located between the helmet CM location of H3- and that of H4- in order to have a balanced head loading. Figure A-1 shows possible locations of the head pivot point for H4- (left diagram) and H3- (right diagram). The rational for these diagrams is that negative loading occurs between H3- and H4-.
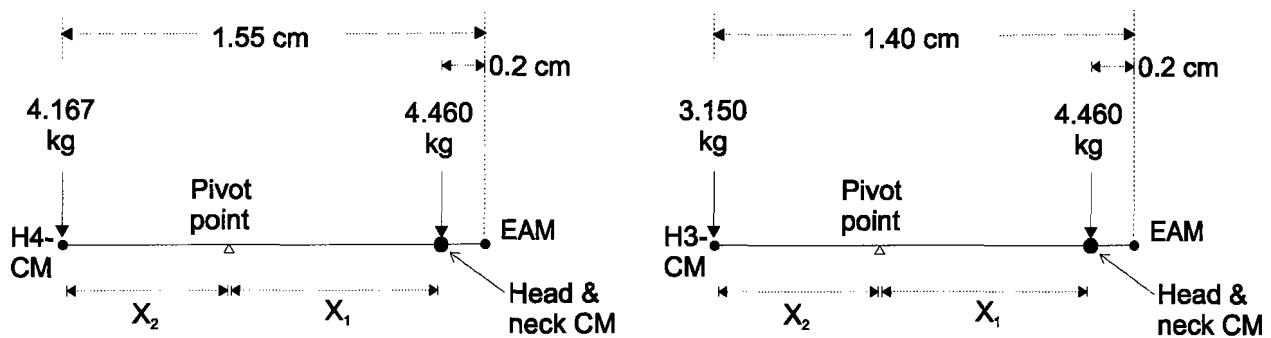
Figure A-1. Head pivot point location in relation to H4- CM (left diagram) and H3- (right diagram). X_1 is the distance between head pivot point and helmet CM. X_2 is the distance between head pivot point and head and neck CM.

Using the regression equations reported by McConville et al. (1980), combined head and neck mass was estimated among the female subjects of this study and found to be 4.46 ± 0.1 kg. For a balanced head-helmet load, the sum of weight moments about the pivot point should be zero, or

$$M_1 \, X_1 - M_2 \, X_2 = 0 \qquad\qquad \text{Equation (A-1)}$$

Where M_1 and X_1 are the combined head and neck mass and CM location relative to pivot point, respectively. M_2 and X_2 are the helmet mass and CM location relative to pivot point, respectively.

Also from Figure A-1,

$$X_1 + X_2 + 0.2 = D \qquad \text{Equation (A-2)}$$

Where D is the distance between helmet CM and head EAM (e.g. 1.55 cm for H4-). Using Equations (A-1) - (A-2) and the values in Figure A-1, X_1 was computed and found to be 0.76 cm for H4- and 0.57 cm for H3-. Therefore, the head pivot point is located between 0.77 and 0.96 cm behind EAM. The location of this functional pivot point is closer than the anatomical pivot point (AOC) identified by Butler (1992), and further than the anatomical one (COC) by Haley and McEntire (1999).

In order to validate this range, future experiments should include subjects with bite bar under sinusoidal vibration at or around resonance with long dwelling time (30-40 sec). The center of head motion can be determined by calculating the best intersection of bite bar position plan during vibration. This location, identified as the functional pivot point, can be compared to the anatomical pivot point determined from the subject's head x-ray with bite bar.
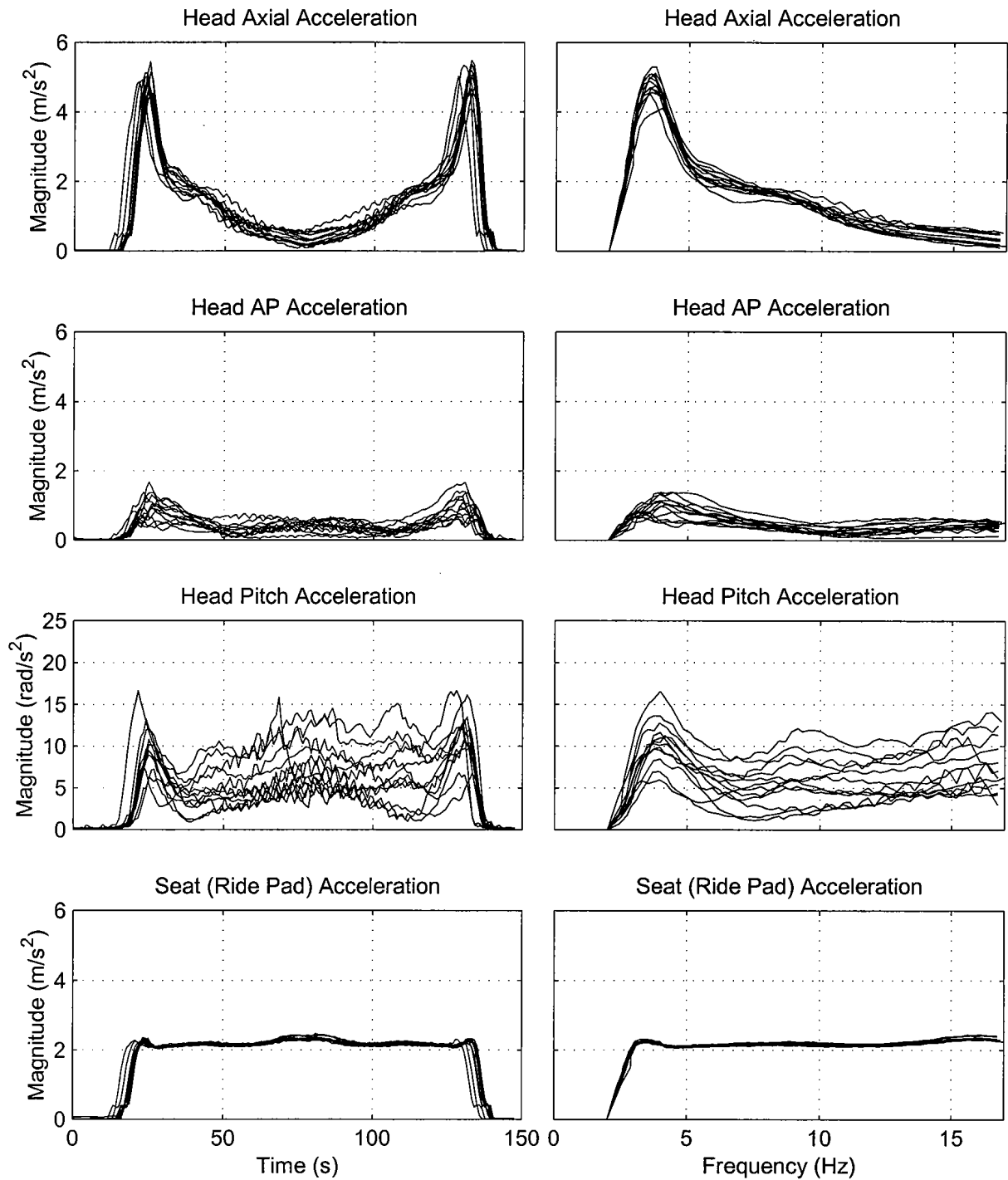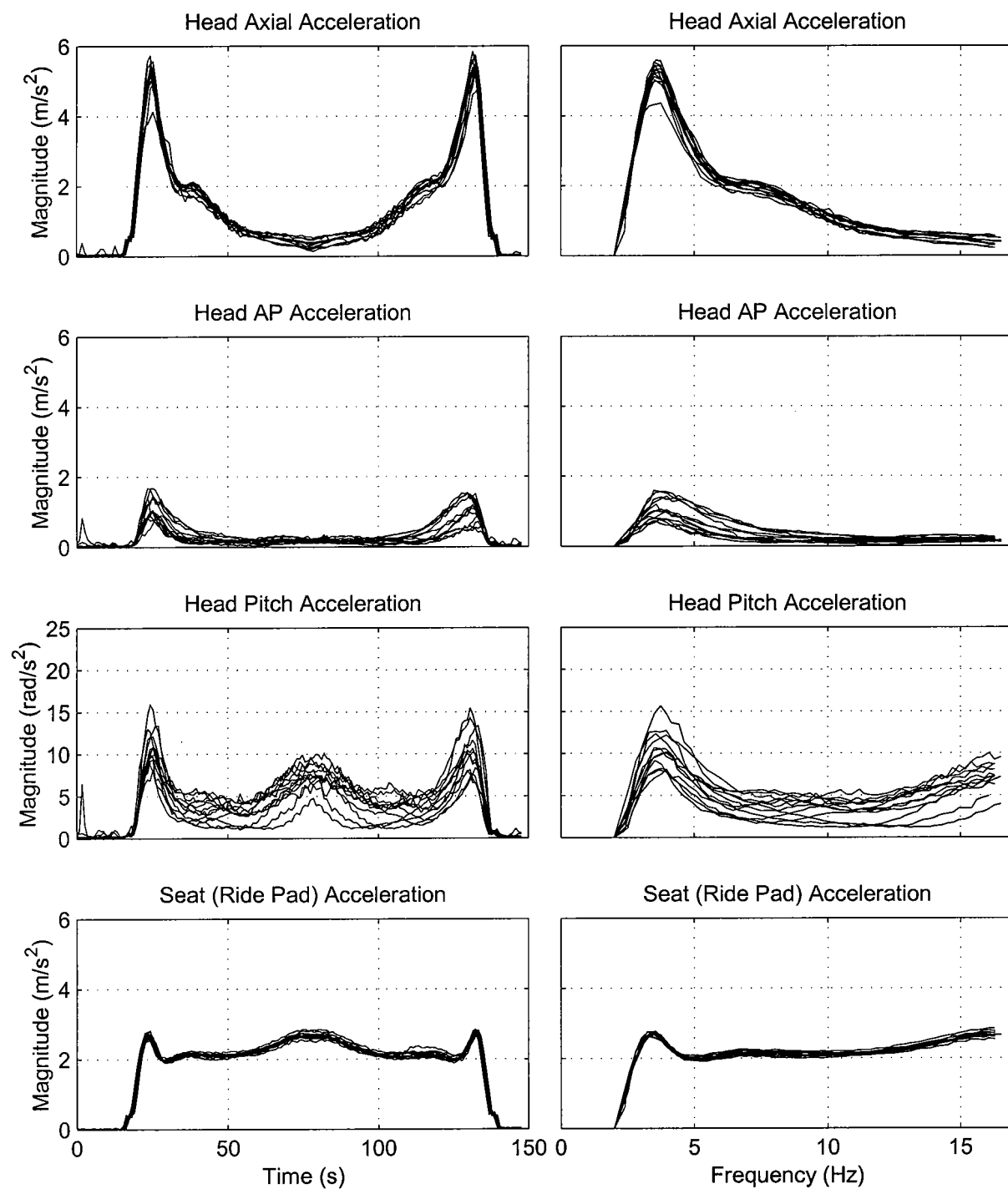
Appendix B.

Figures B-1 through B-12.
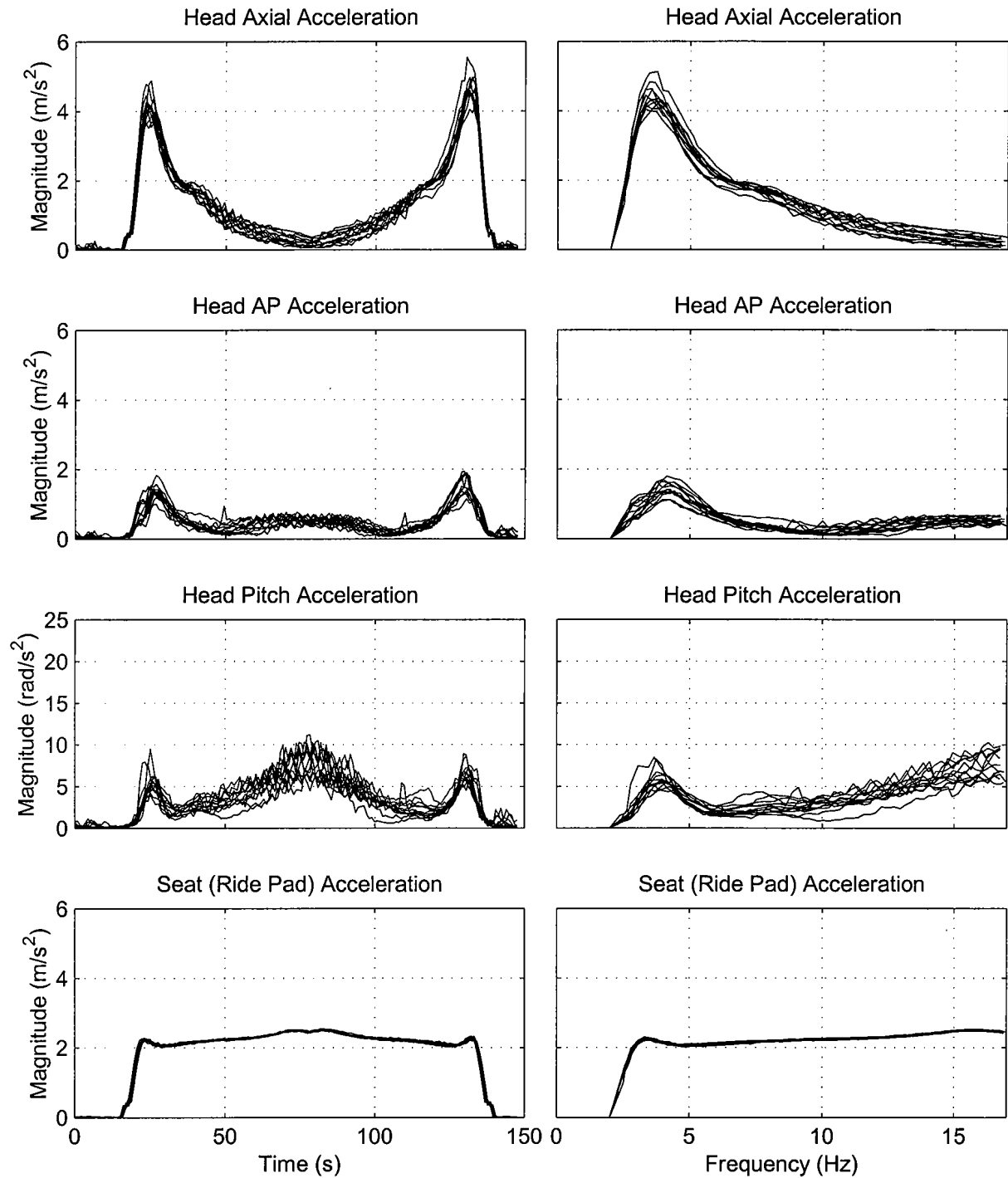
Figure B-1. Head axial, head AP, head pitch, and seat axial accelerations as functions of vibration exposure time (left panels) and as functions of seat vibration frequency (right panels) for subject # 2 over 12 helmet loads.
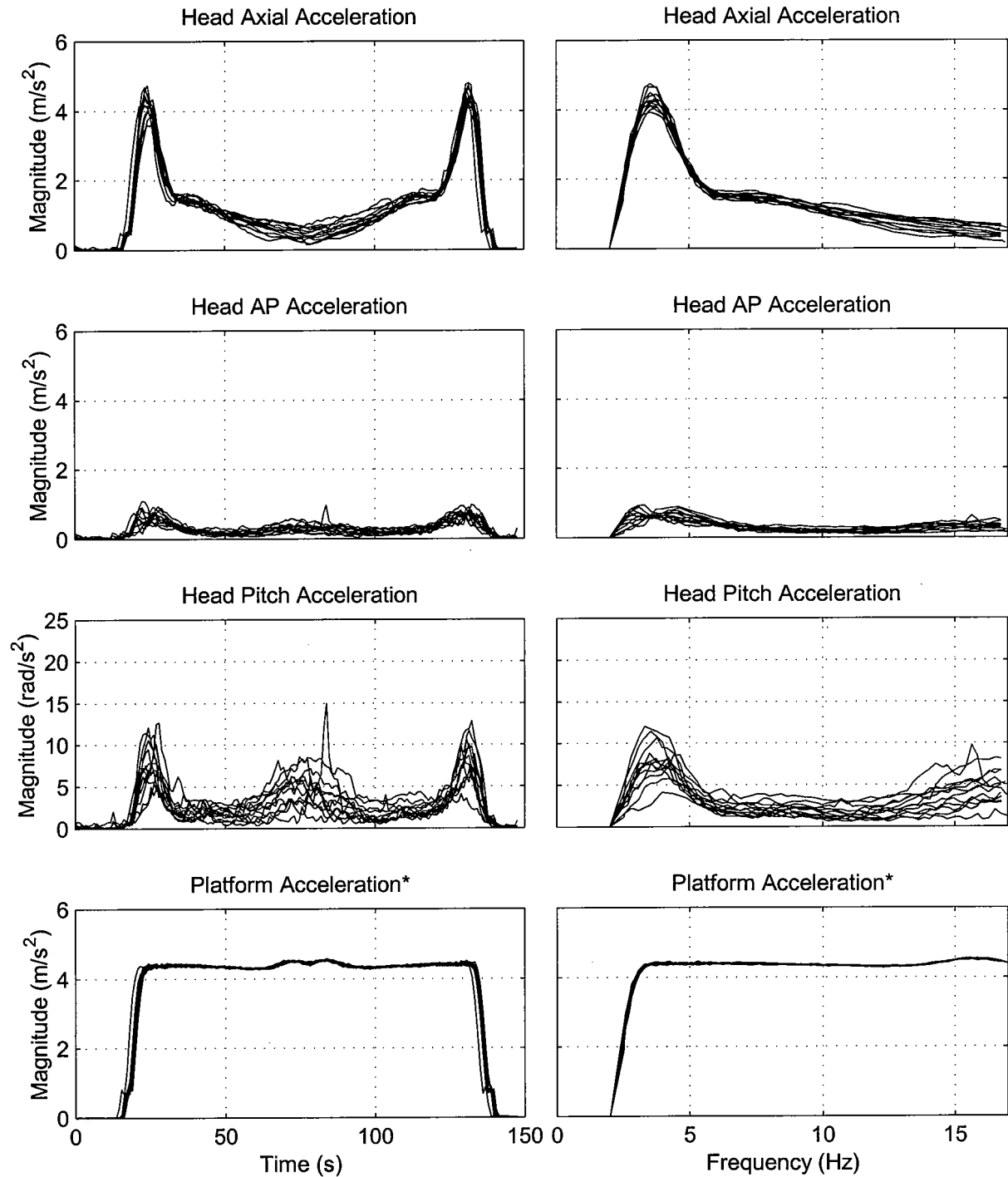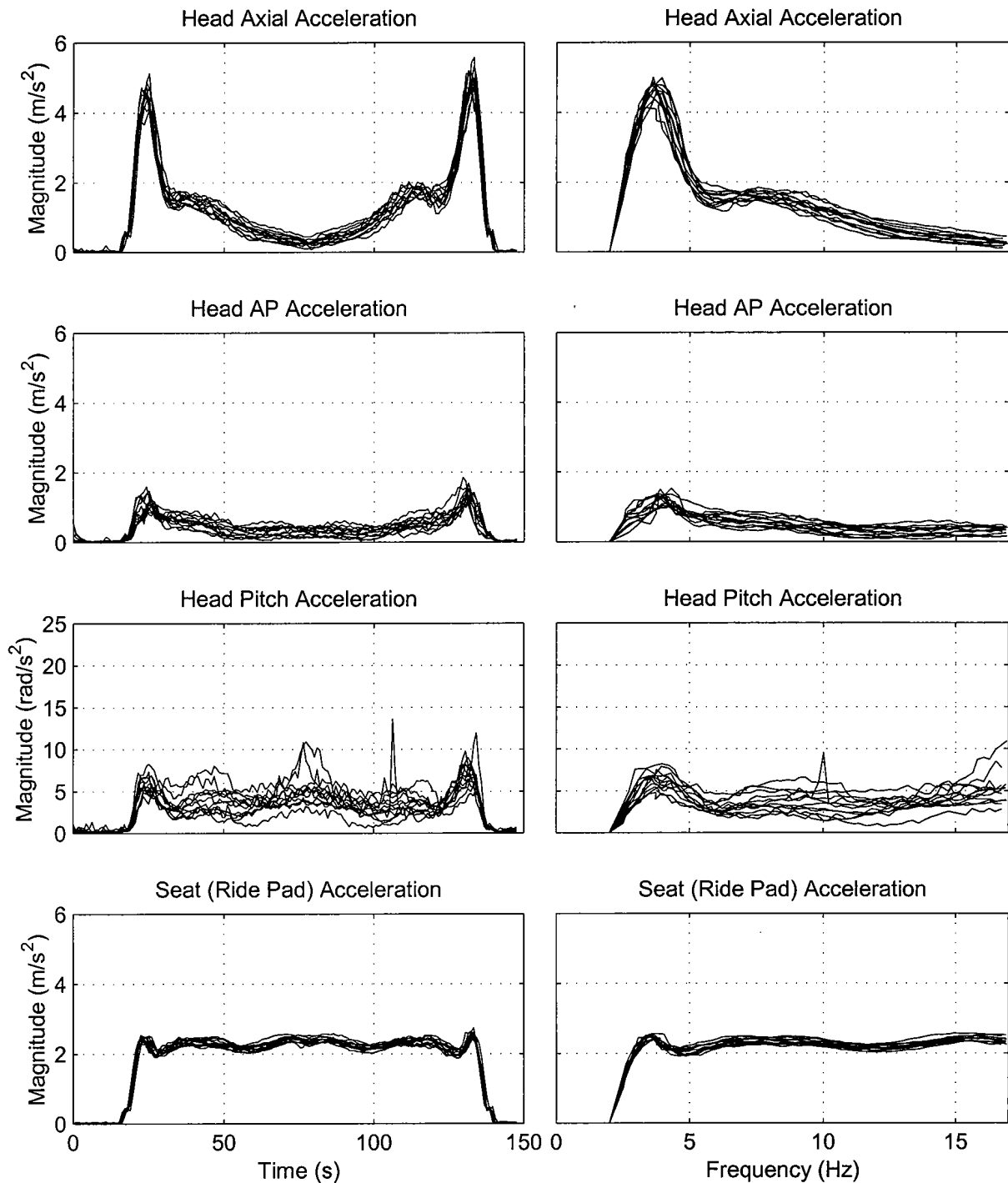
31
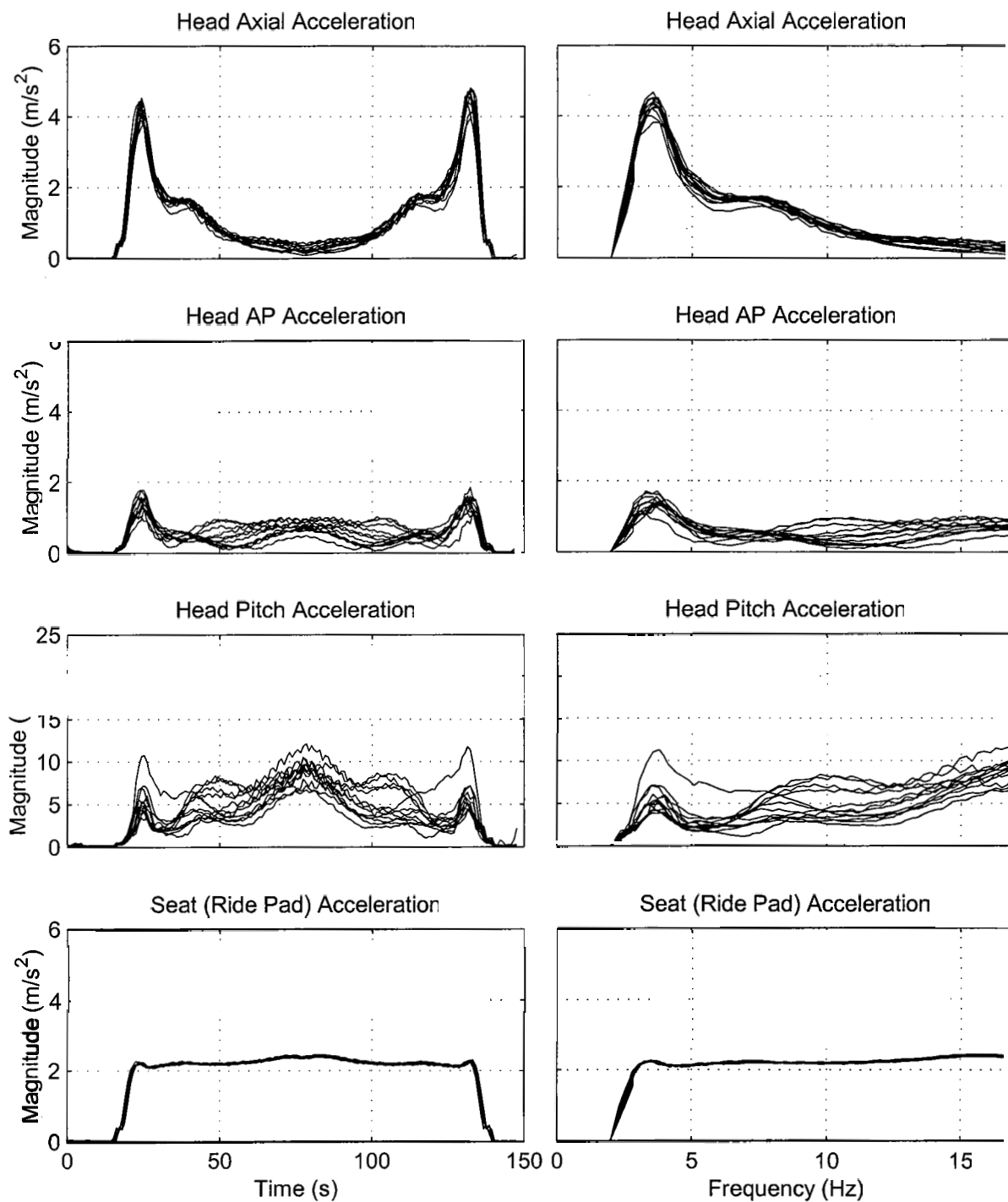
Figure B-2. Head axial, head AP, head pitch, and seat axial accelerations as functions of vibration exposure time (left panels) and as functions of seat vibration frequency (right panels) for subject # 3 over 12 helmet loads.
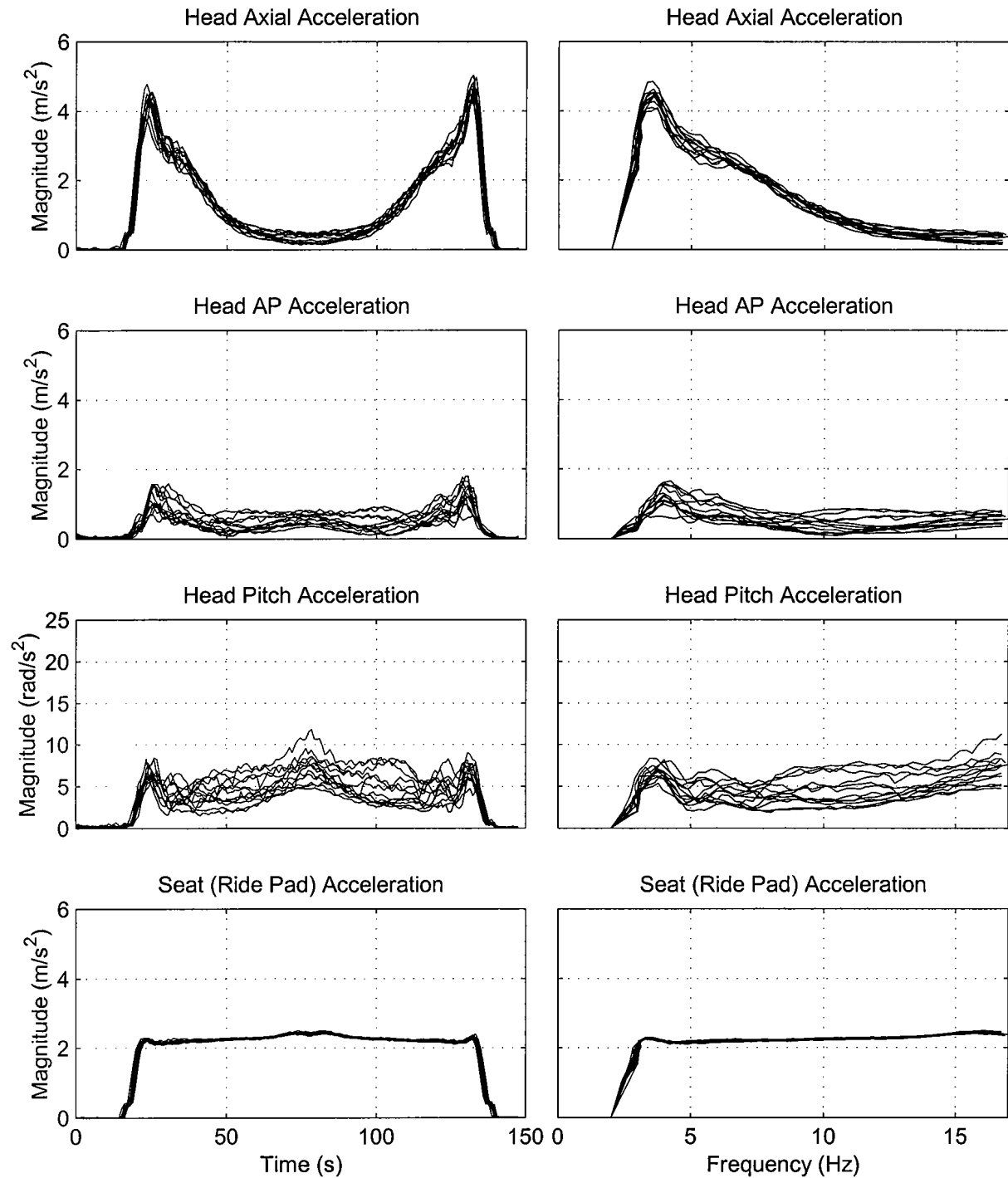
Figure B-3. Head axial, head AP, head pitch, and seat axial accelerations as functions of vibration exposure time (left panels) and as functions of seat vibration frequency (right panels) for subject # 4 over 12 helmet loads.
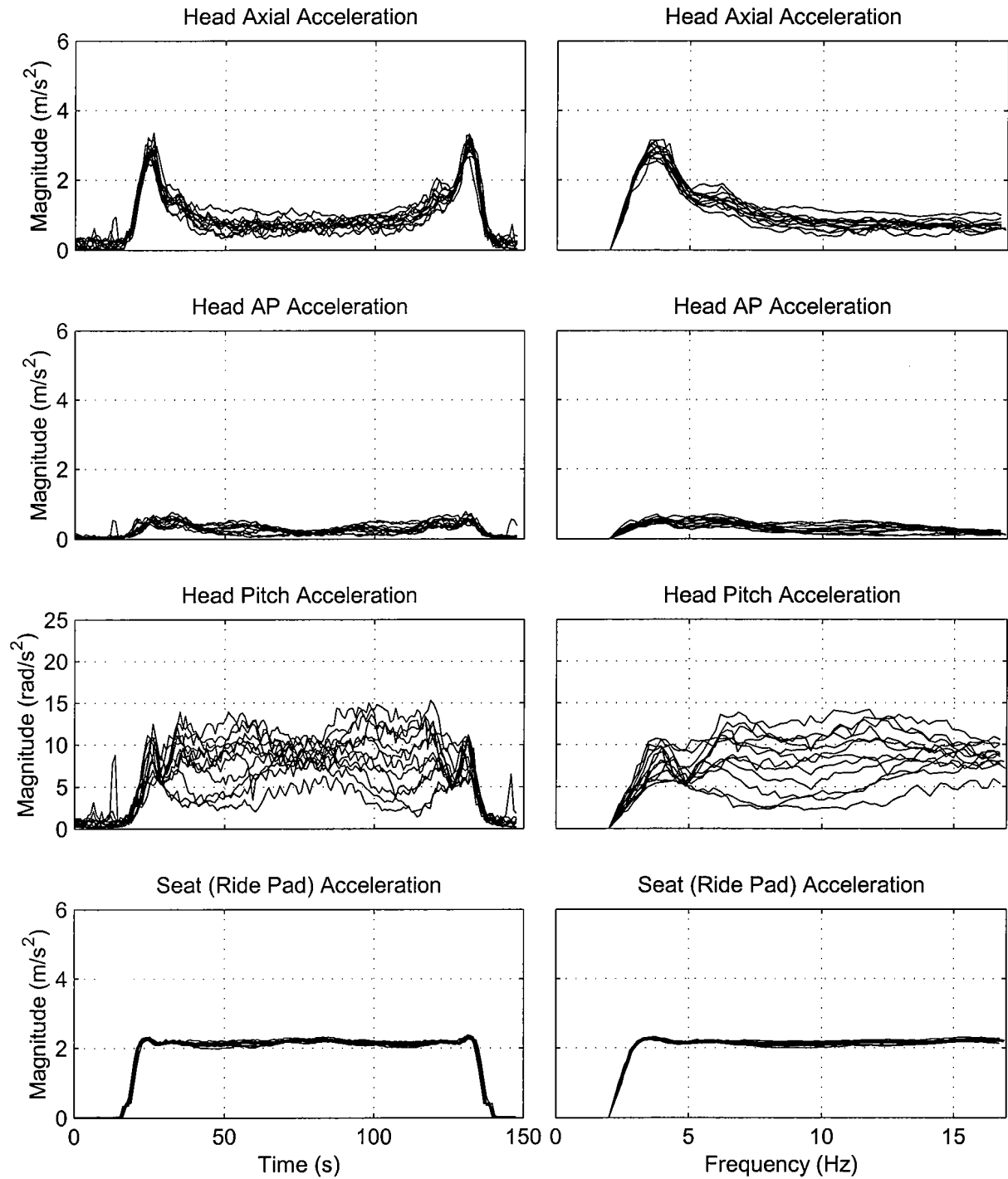
Figure B-4. Head axial, head AP, head pitch, and seat axial accelerations as functions of vibration exposure time (left panels) and as functions of seat vibration frequency (right panels) for subject # 5 over 12 helmet loads.

Figure B-5. Head axial, head AP, head pitch, and seat axial accelerations as functions of vibration exposure time (left panels) and as functions of seat vibration frequency (right panels) for subject # 7 over 12 helmet loads.
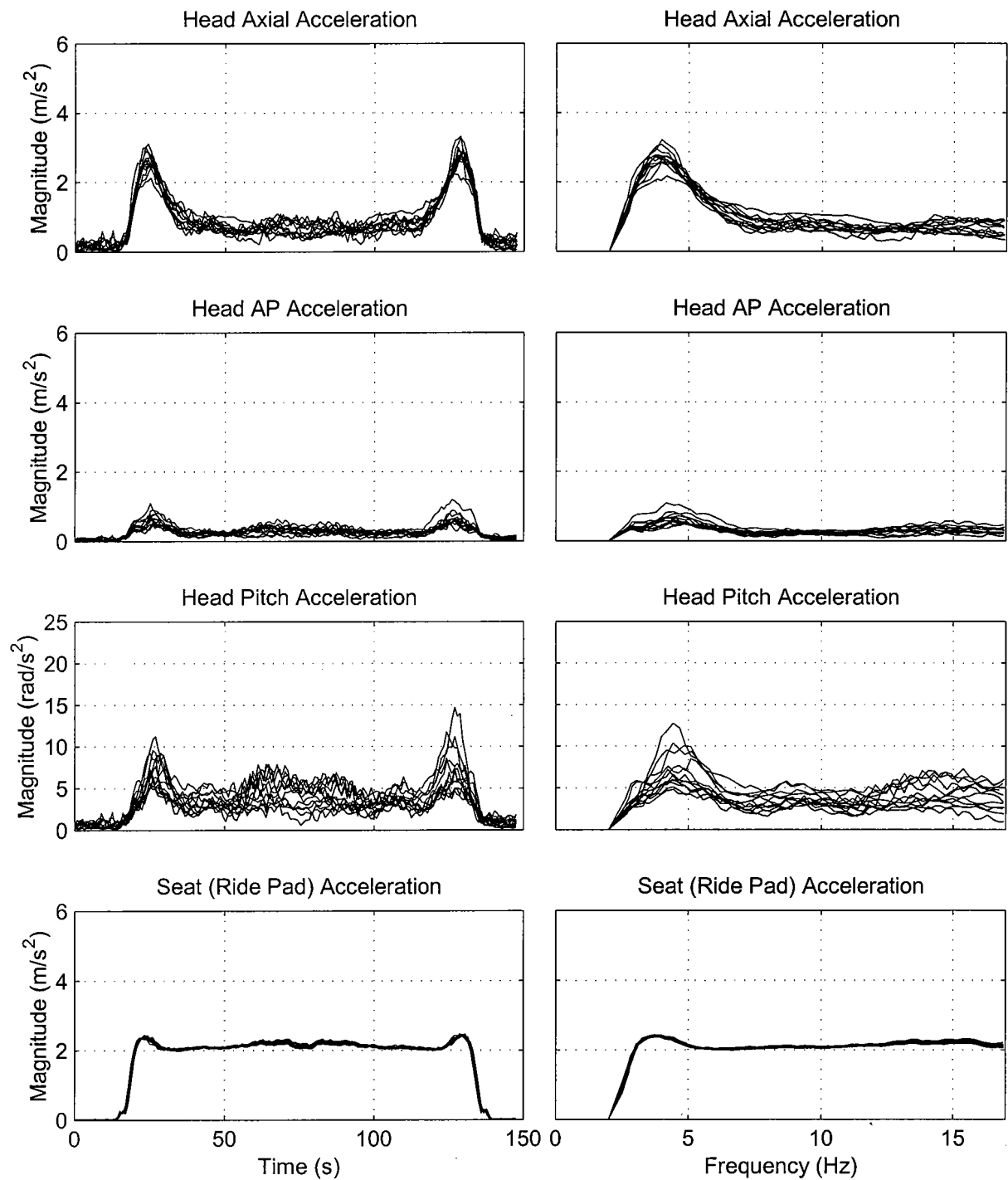
Figure B-6. Head axial, head AP, head pitch, and platform axial accelerations as functions of vibration exposure time (left panels) and as functions of platform vibration frequency (right panels) for subject # 8 over 12 helmet loads. *Seat accelerometer was not operational.
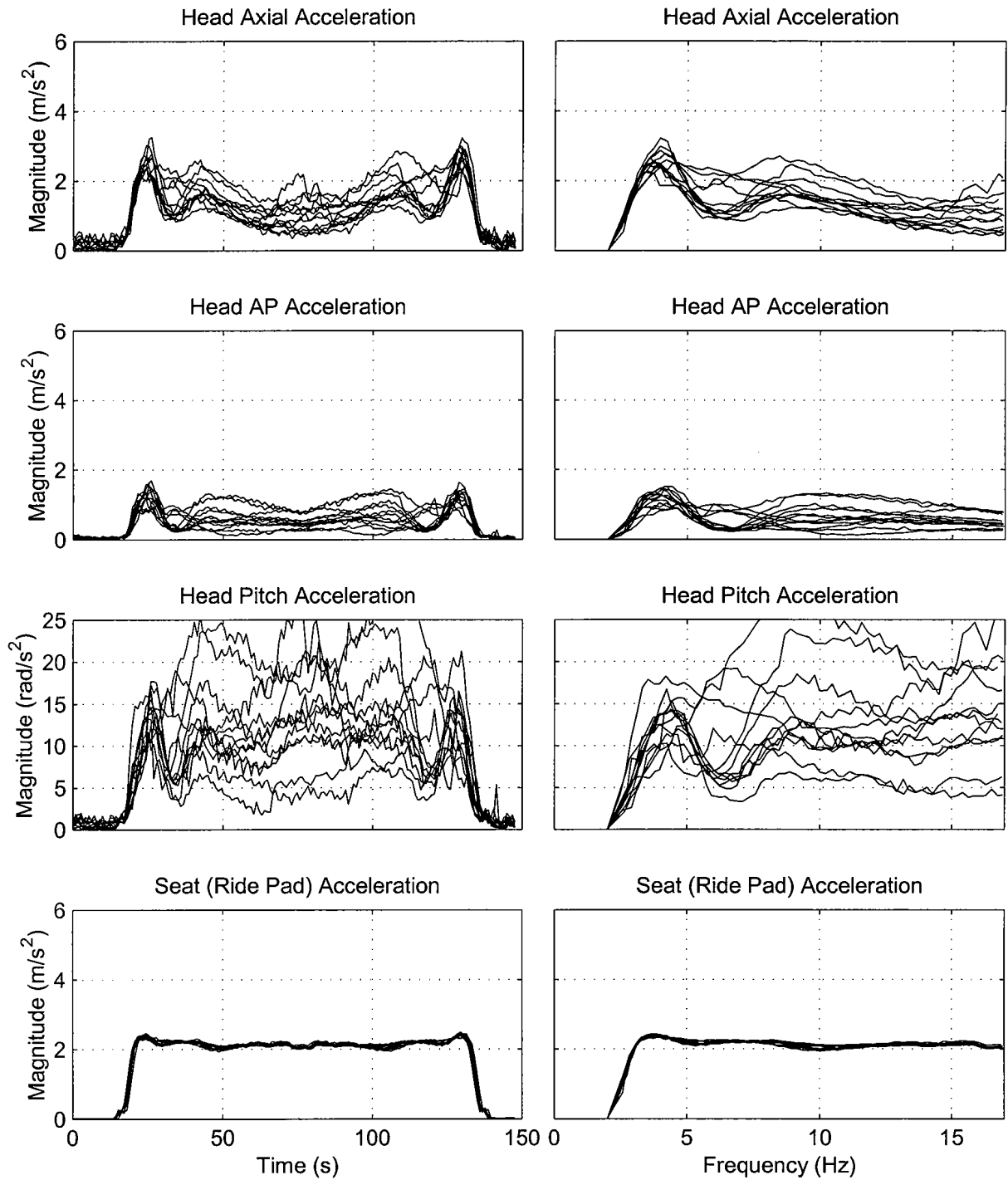
Figure B-7. Head axial, head AP, head pitch, and seat axial accelerations as functions of vibration exposure time (left panels) and as functions of seat vibration frequency (right panels) for subject # 9 over 12 helmet loads.

Figure B-8. Head axial, head AP, head pitch, and seat axial accelerations as functions of vibration exposure time (left panels) and as functions of seat vibration frequency (right panels) for subject # 11 over 12 helmet loads.
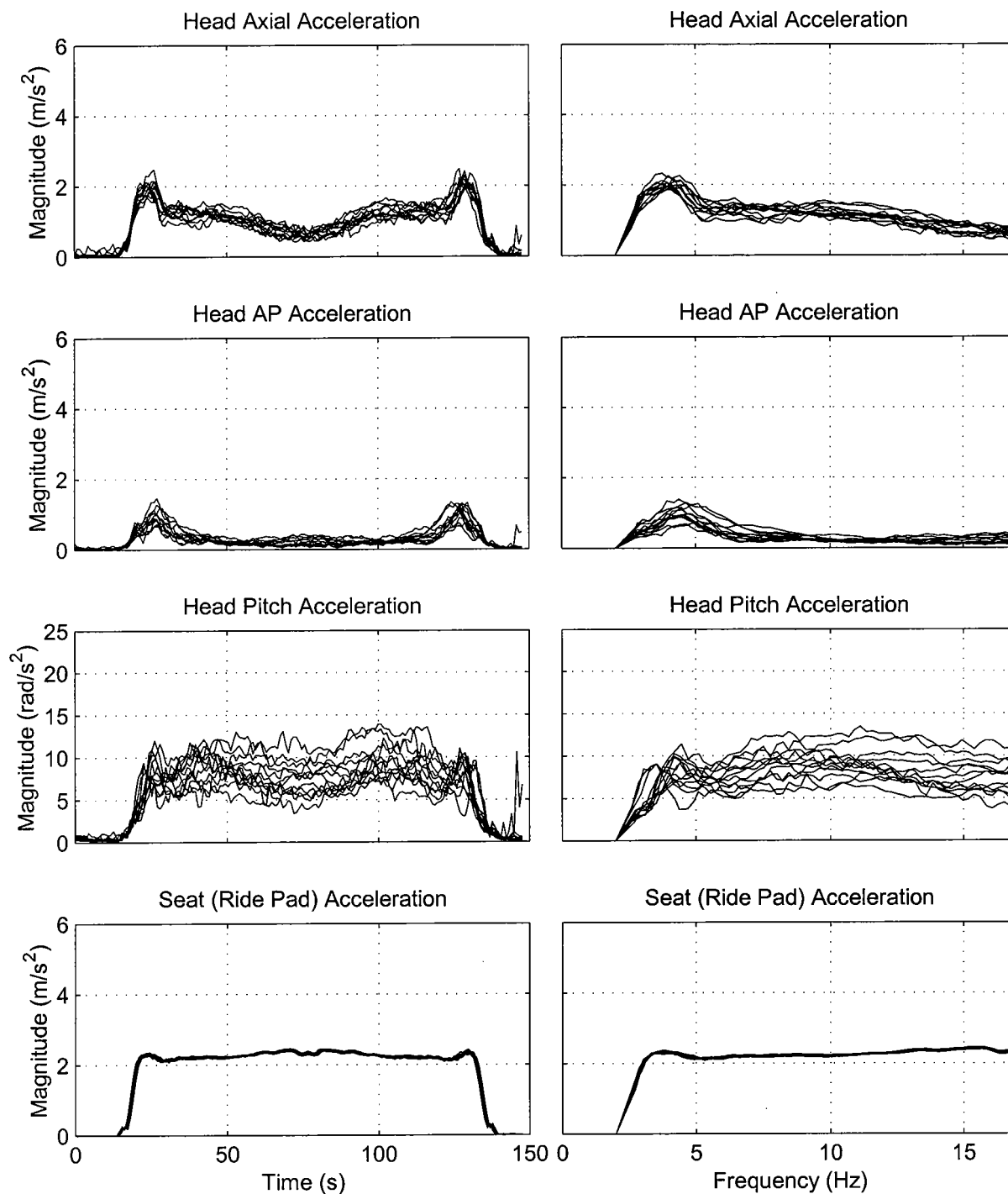
Figure B-9. Head axial, head AP, head pitch, and seat axial accelerations as functions of vibration exposure time (left panels) and as functions of seat vibration frequency (right panels) for subject # 12 over 12 helmet loads.
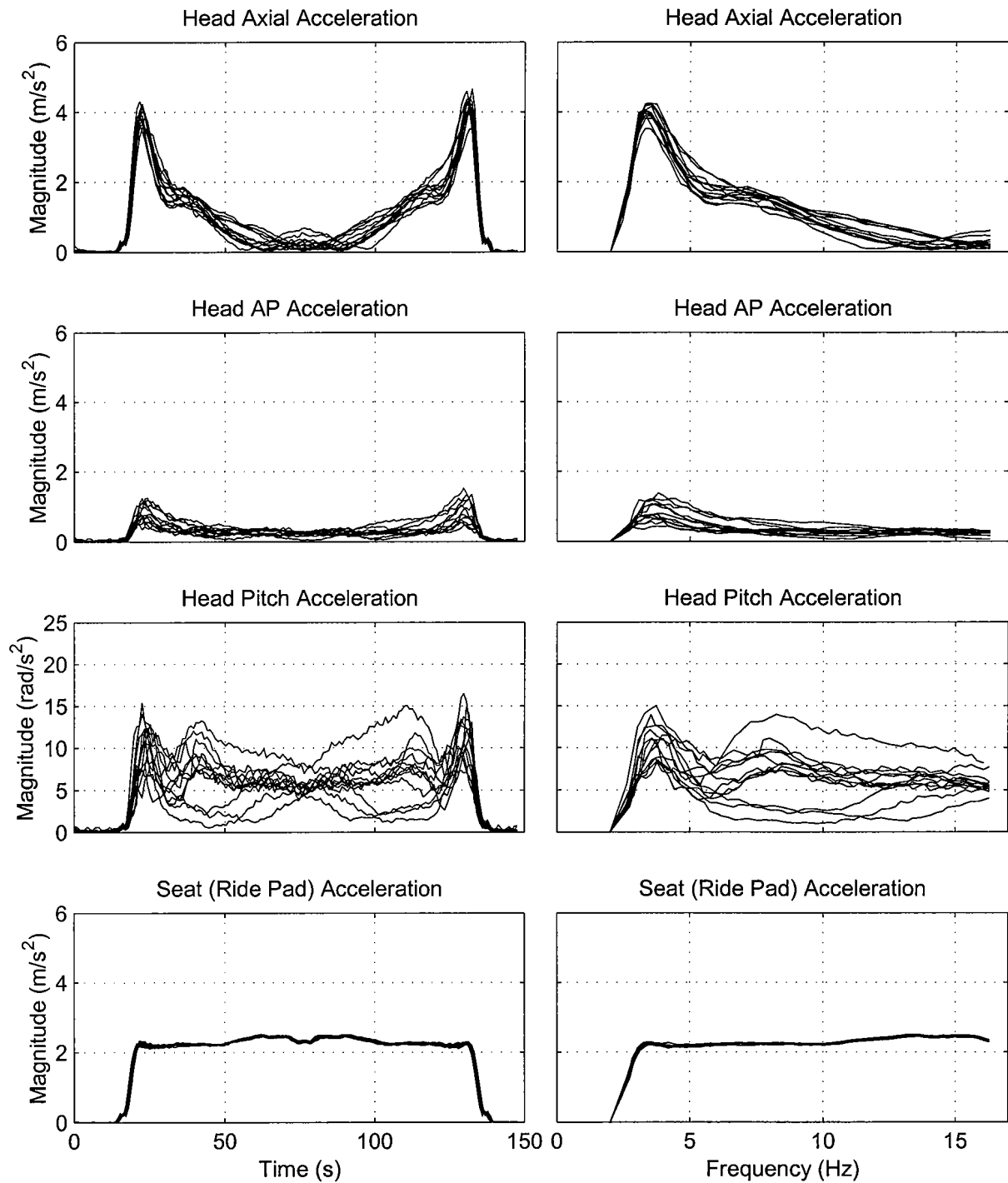
Figure B-10. Head axial, head AP, head pitch, and seat axial accelerations as functions of vibration exposure time (left panels) and as functions of seat vibration frequency (right panels) for subject # 13 over 12 helmet loads.

Figure B-11. Head axial, head AP, head pitch, and seat axial accelerations as functions of vibration exposure time (left panels) and as functions of seat vibration frequency (right panels) for subject # 14 over 12 helmet loads.

Figure B-12. Head axial, head AP, head pitch, and seat axial accelerations as functions of vibration exposure time (left panels) and as functions of seat vibration frequency (right panels) for subject # 15 over 12 helmet loads.
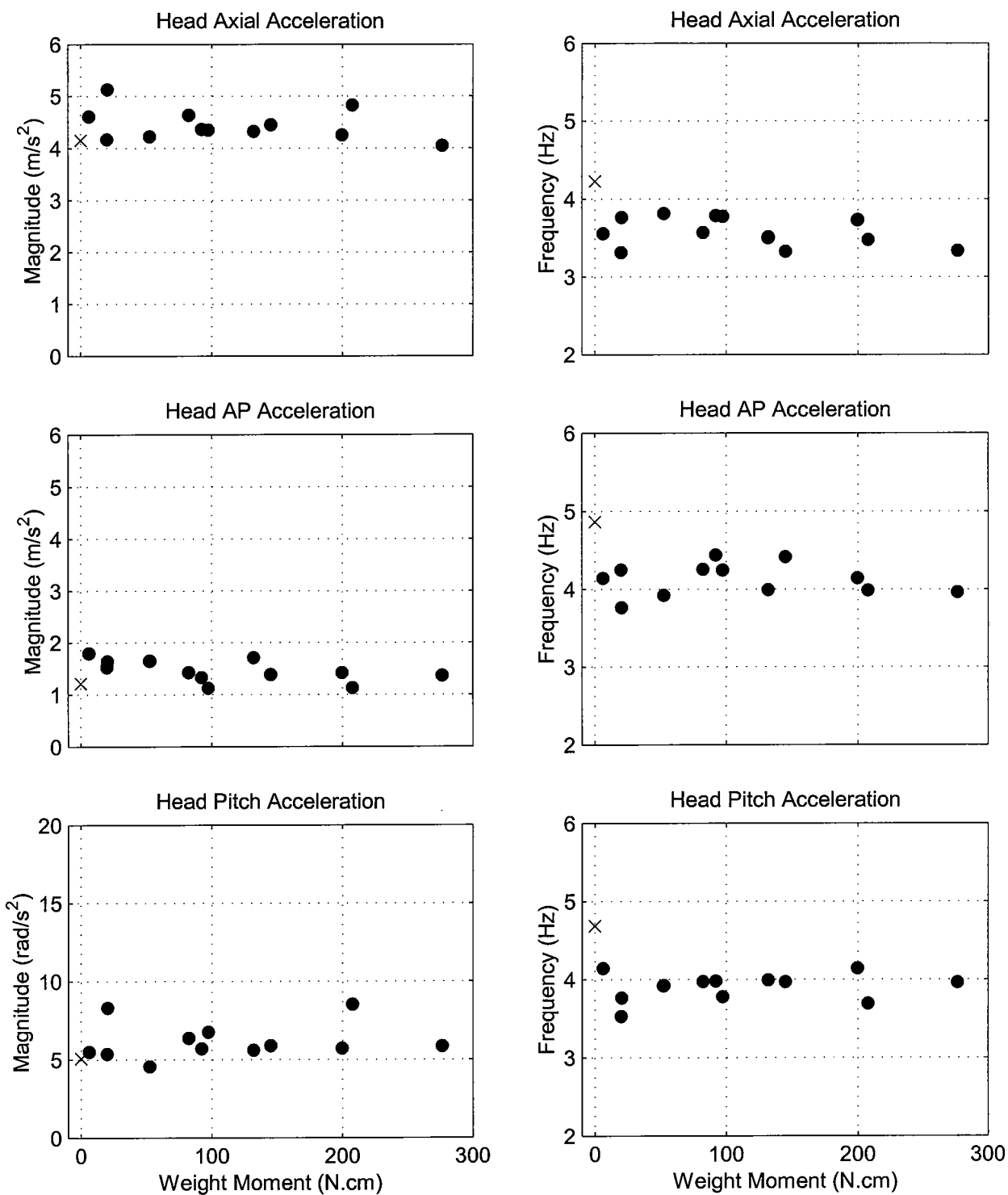
Appendix C.

Figure C-1 through C-12.

Figure C-1. Magnitude and frequency at first resonance for head axial, head AP, and head pitch accelerations plotted as functions of helmet weight moment for subject # 2. The filled circles represent the loaded cases and the "X" represents the unloaded case.
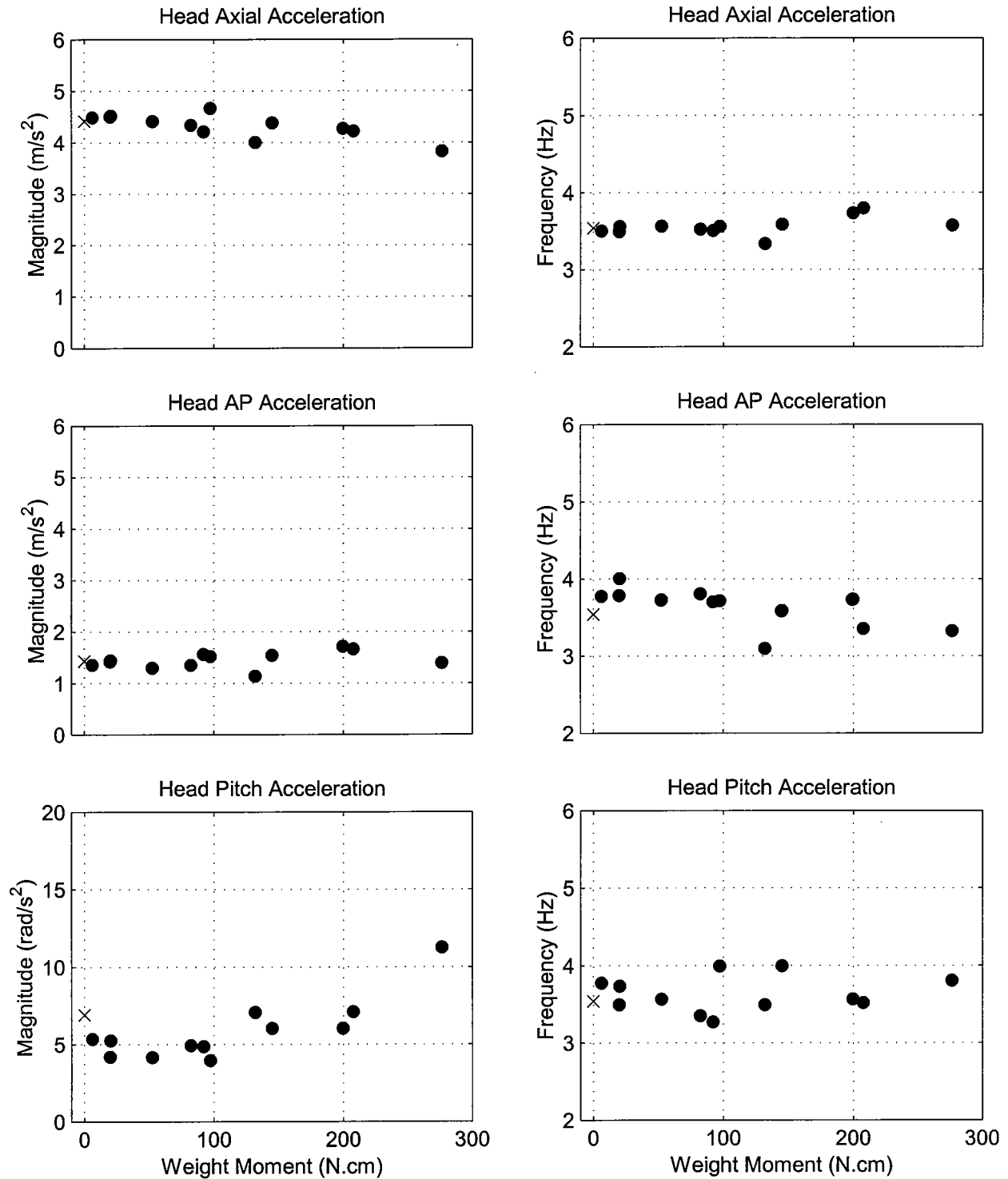
Figure C-2. Magnitude and frequency at first resonance for head axial, head AP, and head pitch accelerations plotted as functions of helmet weight moment for subject # 3. The filled circles represent the loaded cases and the "X" represents the unloaded case.
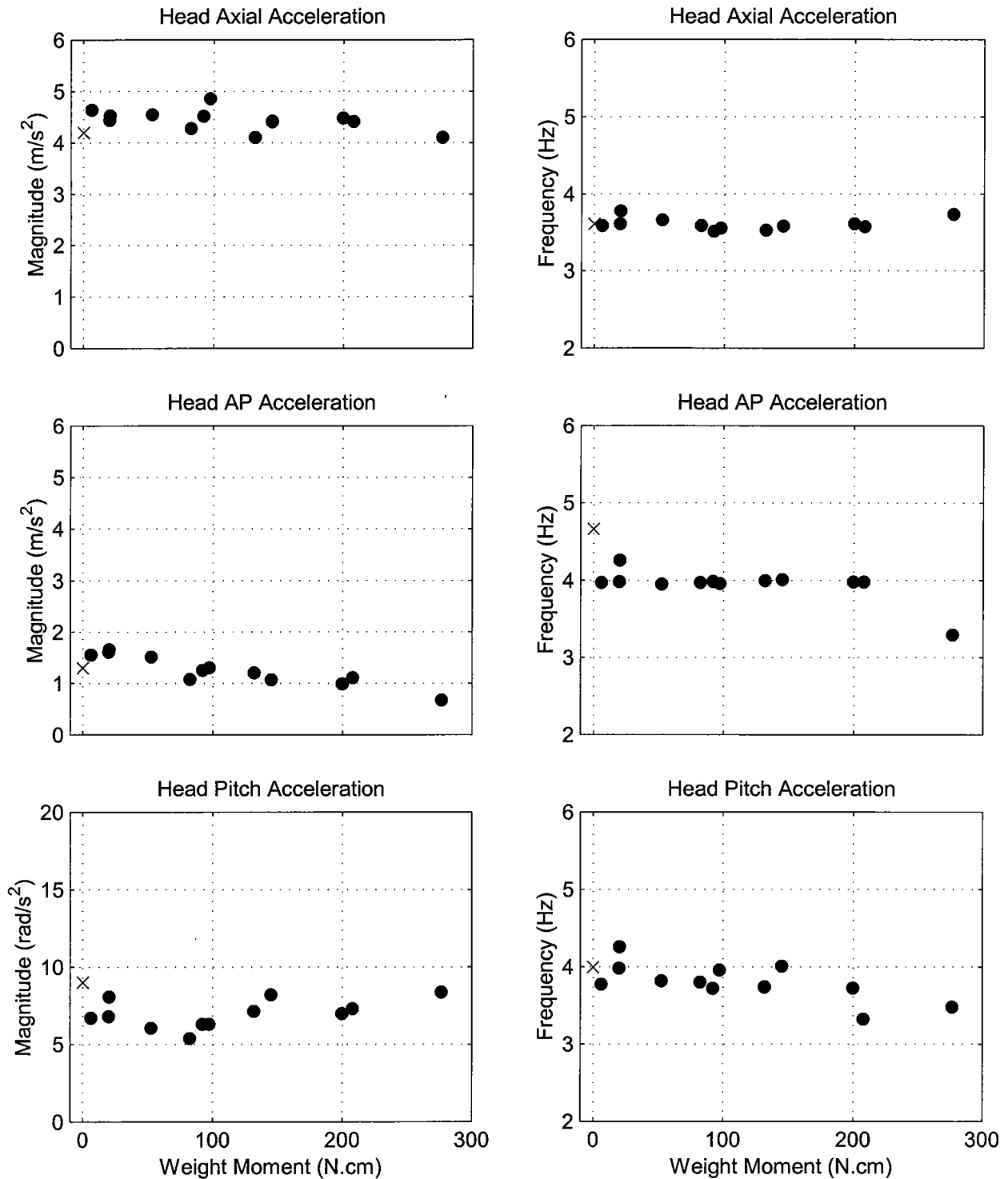
Figure C-3. Magnitude and frequency at first resonance for head axial, head AP, and head pitch accelerations plotted as functions of helmet weight moment for subject # 4. The filled circles represent the loaded cases and the "X" represents the unloaded case.